

## Electronic Supplementary Information (ESI)

### Guanosine-based Hydrogen-bonded Scaffolds: G-ribbons and G-quartets Formed in the Absence of Templating Metal Cation

Mohamed El Garah,<sup>[a]</sup> Rosaria C. Perone,<sup>[b]</sup> Alejandro Santana Bonilla,<sup>[c,d]</sup> Sébastien Haar,<sup>[a]</sup> Marilena Campitiello,<sup>[b]</sup> Rafael Gutierrez,<sup>[c]</sup> Gianauelio Cuniberti,<sup>\*,[c,e]</sup> Stefano Masiero,<sup>\*,[b]</sup> Artur Ciesielski<sup>\*,[a]</sup> and Paolo Samorì<sup>\*,[a]</sup>

- <sup>[a]</sup> Dr. M. El Garah, S. Haar, Dr. A. Ciesielski and Prof. P. Samorì  
ISIS & icFRC, Université de Strasbourg & CNRS, 8 allée Gaspard Monge, 67083 Strasbourg (France)  
E-mail: [ciesielski@unistra.fr](mailto:ciesielski@unistra.fr), [samori@unistra.fr](mailto:samori@unistra.fr)  
Homepage: <http://www.nanochemistry.fr>
- <sup>[b]</sup> Dr. R. C. Perone, M. Campitiello, Prof. S. Masiero  
Alma Mater Studiorum - Università di Bologna, Dipartimento di Chimica "G. CIAMICIAN" Via S. Giacomo 11,  
40126 Bologna (Italy)  
E-mail: [stefano.masiero@unibo.it](mailto:stefano.masiero@unibo.it)
- <sup>[c]</sup> A. Santana Bonilla, Dr. R. Gutierrez, Prof. G. Cuniberti  
Institute for Materials Science and Max Bergmann Center of Biomaterials, Dresden University of Technology, 01062  
Dresden (Germany)
- <sup>[d]</sup> A. Santana Bonilla  
Max Planck Institute for the Physics of Complex Systems  
01187 Dresden (Germany)
- <sup>[e]</sup> Prof. G. Cuniberti  
Center for Advancing Electronics Dresden, Dresden Center for Computational Materials Science, Dresden University  
of Technology, 01062 Dresden (Germany).  
E-mail: [g.cuniberti@tu-dresden.de](mailto:g.cuniberti@tu-dresden.de)

---

## Outline

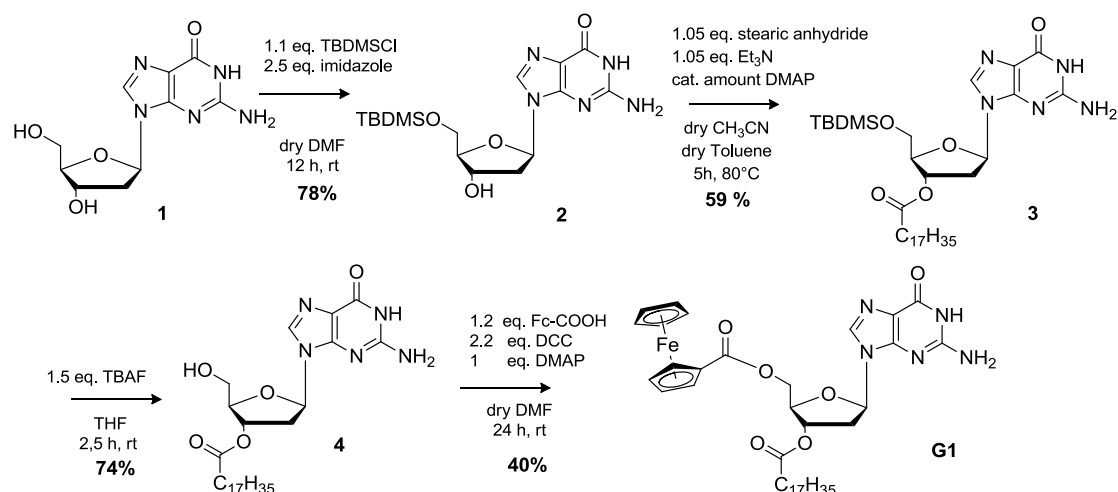
|  |     |
|--|-----|
| 1. <b>Synthesis and characterization</b>   | S2  |
| 1.1 5'- <i>O</i> -ferrocenoyl-3'- <i>O</i> -octadecanoyl-2'-deoxyguanosine ( <b>G1</b> )           | S2  |
| 1.2 8-bromo-5'- <i>O</i> -ferrocenoyl-3'- <i>O</i> -octadecanoyl-2'-deoxyguanosine ( <b>G2</b> )   | S11 |
| 1.3 8-phenoxy-5'- <i>O</i> -ferrocenoyl-3'- <i>O</i> -octadecanoyl-2'-deoxyguanosine ( <b>G3</b> ) | S20 |
| 2. <b>Scanning tunnelling microscopy experiments</b>   | S34 |
| 3. <b>DFT calculations</b>   | S36 |
| 3.1 <b>G1</b> electronic structure   | S36 |
| 3.2 <b>G2</b> electronic structure   | S38 |
| 3.3 <b>G3</b> electronic structure   | S41 |
| References   | S43 |

## 1. Synthesis and characterization

All reactions requiring anhydrous conditions were carried out in oven-dried glassware under dry argon atmosphere. Macherey-Nagel Polygram silica gel plates (layer thickness 0.20 mm) were used for TLC analyses. Column chromatography was performed on Geduran silica gel 60 (40-63  $\mu\text{m}$ ). Reagents and solvents, including dry solvents, were purchased from Aldrich, TCI or Alfa Aesar.

Nuclear magnetic resonance spectra were recorded on Varian (600, 400 or 200 MHz) spectrometers and referenced to the residual solvent resonance (Electrospray ionization mass spectra were obtained from methanol solutions with a Micromass ZMD 4000. CD were recorded with a Jasco J-710 spectropolarimeter (cell path length= 0.01 cm).

### 1.1 5'-O-ferrocenoyl-3'-O-octadecanoyl-2'-deoxyguanosine (G1)



#### 5'-O-tert-butyldimethylsilyl-3'-O-octadecanoyl-2'-deoxyguanosine 3:

Stearic anhydride (1.14 g, 2.07 mmol) and a catalytic amount of 4-dimethylamino pyridine (DMAP) were added to a flask containing a suspension of 5'-O-tert-butyldimethylsilyl-2'-deoxyguanosine **2**<sup>1</sup> (750 mg, 1.97 mmol, dried over P<sub>2</sub>O<sub>5</sub> *in vacuo* for 2 h at 60 °C) in 30 mL of an acetonitrile - toluene mixture 1:1 and triethylamine (TEA) (288  $\mu\text{L}$ , 2.07mmol). The reaction was stirred at 80° C under argon for 5 h. The solvents were removed under reduced pressure and the crude material was dissolved in dichloromethane and extracted three times with a saturated solution of NaHCO<sub>3</sub>. The organic layer was then dried over MgSO<sub>4</sub>. The crude material was purified by column chromatography on silica gel using ether to elute stearic acid, then with dichloromethane/ methanol (95:5) as eluent to afford the desired product as a white solid (750 mg, 1.16 mmol, yield 59%).

ESI-MS (positive mode, MeOH solution,  $m/z$ ): 648.1 [M+H]<sup>+</sup>, 670.3 [M+Na]<sup>+</sup>.

<sup>1</sup> M. Iurlo, L. Mengozzi, S. Rapino, M. Marcaccio, R. C. Perone, S. Masiero, P.G. Cozzi, F. Paolucci, *Organometallics*, 2014, **33**(18), 4986-4993

---

IR (KBr): 3458, 3308, 3197, 2915, 2863, 1737, 1260  $\text{cm}^{-1}$ .

$^1\text{H-NMR}$   $\delta$  (dms $\text{-d}_6$ ): 0.030 (s, 3H, SiMe), 0.040 (s, 3H, SiMe), 0.847 (t, 3H, Me), 0.853 (s, 9H, tBu), 1.21-1.28 (m, 28H,  $\text{CH}_2$ ), 1.538 (qi,  $J=7.2$ , 2H,  $-\text{CO}-\text{CH}_2-\text{CH}_2-$ ), 2.340 (t,  $J=7.2$ , 2H,  $-\text{CO}-\text{CH}_2-$ ), 2.405 (ddd,  $J=13.8, 5.9, 1.7$ , 1H,  $\text{H}^{2'}$ ), 2.764 (ddd,  $J=13.8, 8.4, 6.6$ , 1H,  $\text{H}^{2'}$ ), 3.758 (m, 2H,  $\text{CH}_2^{5'}$ ), 4.003 (m, 1H,  $\text{H}^{4'}$ ), 5.293 (m, 1H,  $\text{H}^{3'}$ ), 6.103 (dd,  $J=8.4, 5.9$ , 1H,  $\text{H}^{1'}$ ), 6.515 (bs, 2H,  $\text{NH}_2$ ), 7.856 (s, 1H,  $\text{H}^8$ ), 10.711 (bs, 1H, NH) ppm.

$^{13}\text{C-NMR}$   $\delta$  (dms $\text{-d}_6$ ): Elemental analysis calcd (%) for  $\text{C}_{34}\text{H}_{61}\text{N}_5\text{O}_5\text{Si}$ : C 63.02, H 9.49, N 10.81; found: C 63.12, H 9.49, N 10.78.

### 3'-O-octadecanoyl-2'-deoxyguanosine 4

Tetrabutylammonium fluoride trihydrate (TBAF) (547 mg, 1.73 mmol) was added to a solution of 5'-O-tert-butyldimethylsilyl-3'-O-octadecanoyl-deoxyguanosine (750 mg, 1.16 mmol) in THF (20 mL) and the solution was stirred for 4 h at room temperature. The solvent was removed under reduced pressure and the crude material was dissolved in dichloromethane and extracted three times with water. The organic layer was then dried over  $\text{MgSO}_4$ . The crude material was purified by column chromatography on silica gel using dichloromethane /methanol (96:4) as eluent, affording the product as a white solid (460 mg, 0.85 mmol, yield 74%)

ESI-MS (positive mode, MeOH solution,  $m/z$ ): 534.2  $[\text{M}+\text{H}]^+$ , 567.3  $[\text{M}+\text{Na}]^+$ .

IR (KBr): 3307, 3176, 2928, 2875, 1733  $\text{cm}^{-1}$ .

$^1\text{H-NMR}$   $\delta$  (dms $\text{-d}_6$ ): 0.847 (t,  $J=7.2$ , 3H, Me), 1.245 (m, 28H,  $\text{CH}_2$ ), 1.520 (qi,  $J=7.2$ , 2H,  $-\text{CO}-\text{CH}_2-\text{CH}_2-$ ), 2.340 (t,  $J=7.2$ , 2H,  $-\text{CO}-\text{CH}_2-$ ), 2.371 (m, 1H,  $\text{H}^{2'}$ ), 2.771 (m, 1H,  $\text{H}^{2'}$ ), 3.596 (m, 2H,  $\text{CH}_2^{5'}$ ), 3.988 (m, 1H,  $\text{H}^{4'}$ ), 5.122 (t,  $J=5.6$ , 1H, OH), 5.308 (m, 1H,  $\text{H}^{3'}$ ), 6.104 (dd,  $J=9.6, 5.8$ , 1H,  $\text{H}^{1'}$ ), 6.474 (bs, 2H,  $\text{NH}_2$ ), 7.950 (s, 1H,  $\text{H}^8$ ), 10.642 (bs, 1H, NH) ppm.

$^{13}\text{C-NMR}$   $\delta$  (dms $\text{-d}_6$ ): 14.423, 22.598, 24.810, Elemental analysis calcd (%) for  $\text{C}_{28}\text{H}_{47}\text{N}_5\text{O}_5$ : C 63.01, H 8.88, N 13.12; found: C 63.08, H 8.88, N 13.11.

### 5'-O-ferrocenoyl-3'-O-octadecanoyl-2'-deoxyguanosine G1

Ferrocene carboxylic acid (238 mg, 1.03 mmol) and 3'-O-decanoyl-2'-deoxyguanosine (460 mg, 0.86 mmol) were dried over  $\text{P}_2\text{O}_5$  *in vacuo* for 2 h at 60 °C. Ferrocene carboxylic acid was then dissolved in DMF (10 mL), DCC (467 mg, 2.27 mmol) was added and the resulting solution was stirred under argon atmosphere. After 30 min. 3'-O-decanoyl-2'-deoxyguanosine and DMAP (126 mg, 1.03 mmol) were added and the solution was stirred for 4 h. The solvent was removed under reduced pressure, the crude was dissolved in dichloromethane and extracted with a sat.  $\text{NaHCO}_3$ . The organic layer was dried over  $\text{MgSO}_4$ . The reaction mixture was applied to a silica gel column packed in

---

dichloromethane and eluted with a gradient of methanol in dichloromethane. The final product was eluted with a mixture of dichloromethane-methanol (96:4) yielding the product as a yellow solid (260 mg, 0.35 mmol, yield 40%).

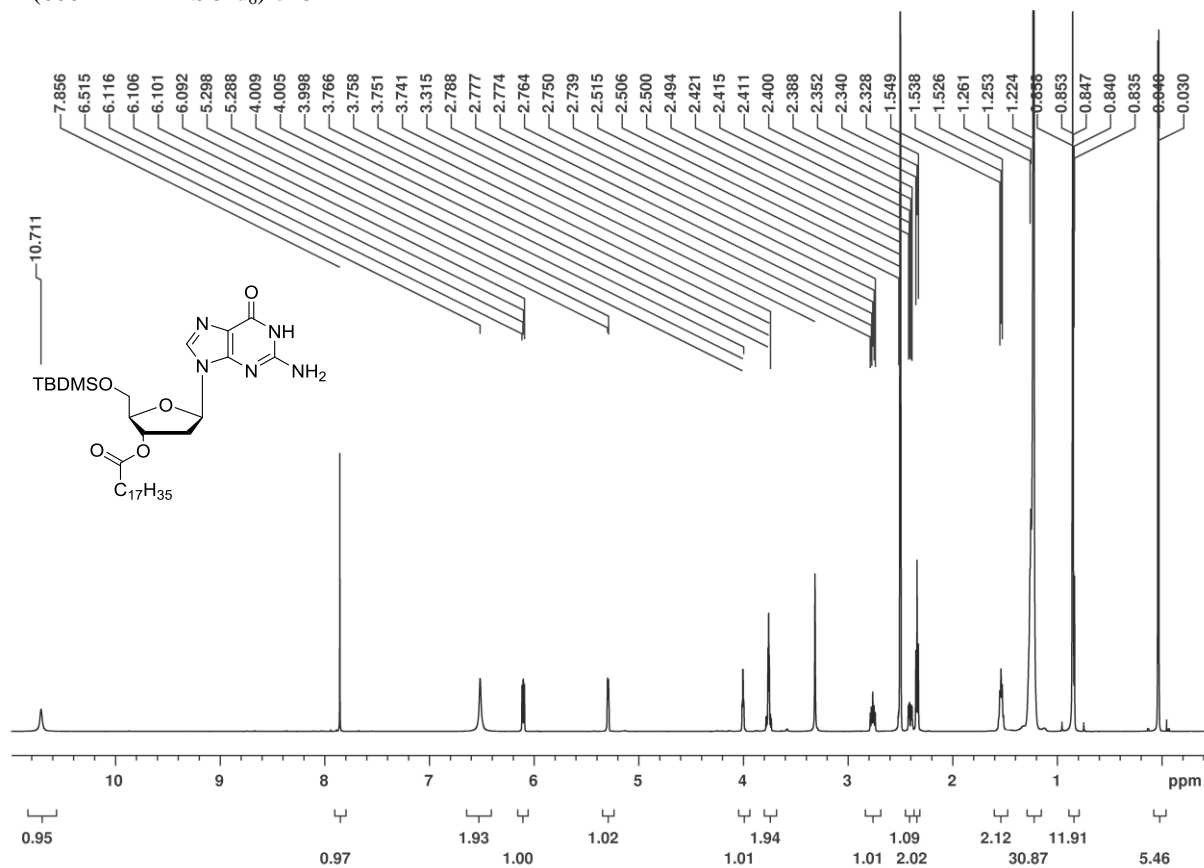
ESI-MS (positive mode, MeOH solution,  $m/z$ ): 746.7  $[M+H]^+$ , 768.5  $[M+Na]^+$ .

IR (KBr): 3413, 3308, 3157, 2951, 2868, 1736, 1682, 492  $\text{cm}^{-1}$ .

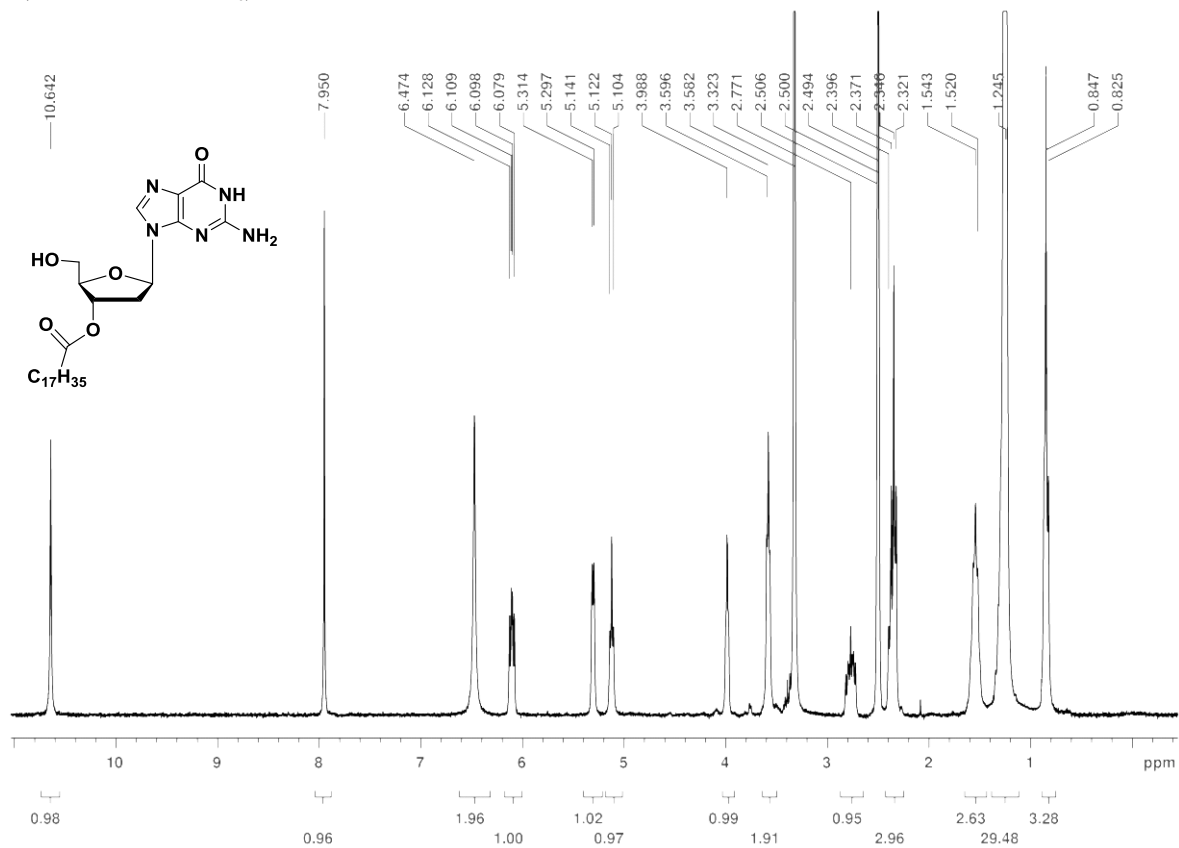
$^1\text{H-NMR}$   $\delta$  (dms $\text{-d}_6$ ): 0.849 (t,  $J=6.6$ , 3H, Me), 1.222 (m, 28H,  $\text{CH}_2$ ), 1.556 (qi,  $J=7.2$ , 2H,  $-\text{CO}-\text{CH}_2-\text{CH}_2-$ ), 2.375 (t,  $J=7.2$ , 2H,  $-\text{CO}-\text{CH}_2-$ ), 2.515 (m, 1H,  $\text{H}^{2'}$ ), 2.983 (m, 1H,  $\text{H}^{2'}$ ), 4.191 (s, 5H,  $\text{Fc-C}_5\text{H}_5$ ), 4.290 (dt,  $J=5.2$ , 1.9, 1H,  $\text{H}^{4'}$ ), 4.330 (dd,  $J=11.4$ , 5.2, 1H,  $\text{H}^{5'}$ ), 4.426 (dd,  $J=11.4$ , 5.2, 1H,  $\text{H}^{5'}$ ), 4.498 (m, 2H,  $\text{Fc-C}_5\text{H}_4$ ), 4.749 (m, 2H,  $\text{Fc-C}_5\text{H}_4$ ), 5.415 (m, 1H,  $\text{H}^{3'}$ ), 6.183 (dd,  $J=9.0$ , 6.0, 1H,  $\text{H}^{1'}$ ), 6.478 (bs, 2H,  $\text{NH}_2$ ), 7.959 (s, 1H,  $\text{H}^8$ ), 10.646 (bs, 1H, NH) ppm.

$^{13}\text{C-NMR}$   $\delta$  (dms $\text{-d}_6$ ): 14.420 (Me), 22.555 ( $\text{CH}_2$ ), 24.769 ( $-\text{CO}-\text{CH}_2-\text{CH}_2-$ ), 28.872 ( $\text{CH}_2$ ), 29.142 ( $\text{CH}_2$ ), 29.161 ( $\text{CH}_2$ ), 29.325 ( $\text{CH}_2$ ), 29.421 ( $\text{CH}_2$ ), 29.453 ( $\text{CH}_2$ ), 29.479 ( $\text{CH}_2$ ), 29.494 ( $\text{CH}_2$ ), 31.752 ( $\text{CH}_2$ ), 33.907 ( $-\text{CO}-\text{CH}_2-$ ), 36.253 ( $\text{C}^{2'}$ ), 63.940 ( $\text{C}^{5'}$ ), 70.073 ( $\text{Fc-C}_5\text{H}_5$ ), 70.234 and, 70.319 ( $\text{Fc-C}_5\text{H}_4$ ), 70.582 ( $\text{Fc-C}^{\text{IV}}-\text{CO}$ ), 72.017 and 72.030 ( $\text{Fc-C}_5\text{H}_4$ ), 74.728 ( $\text{C}^{3'}$ ), 82.047 ( $\text{C}^{4'}$ ), 83.255 ( $\text{C}^{1'}$ ), 117.339 (C5), 135.508 (C8), 151.529 (C4), 154.226, 157.139, 170.906 (CO-Fc), 172.992 ( $\text{CO}-\text{CH}_2$ ) ppm. Elemental analysis calcd (%) for  $\text{C}_{39}\text{H}_{55}\text{FeN}_5\text{O}_6$ : C 62.81, H 7.43, N 9.39; found: C 62.72, H 7.45, N 9.40.

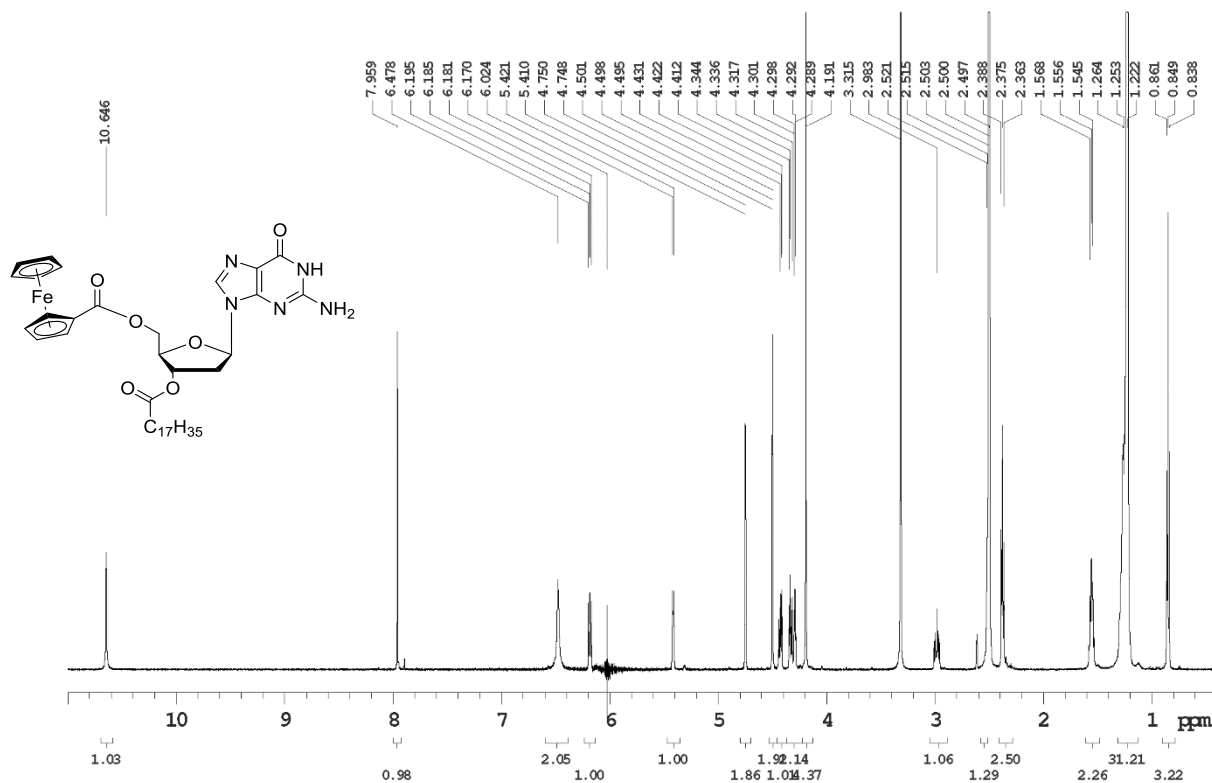
H-NMR (600 MHz DMSO-d<sub>6</sub>) of **3**



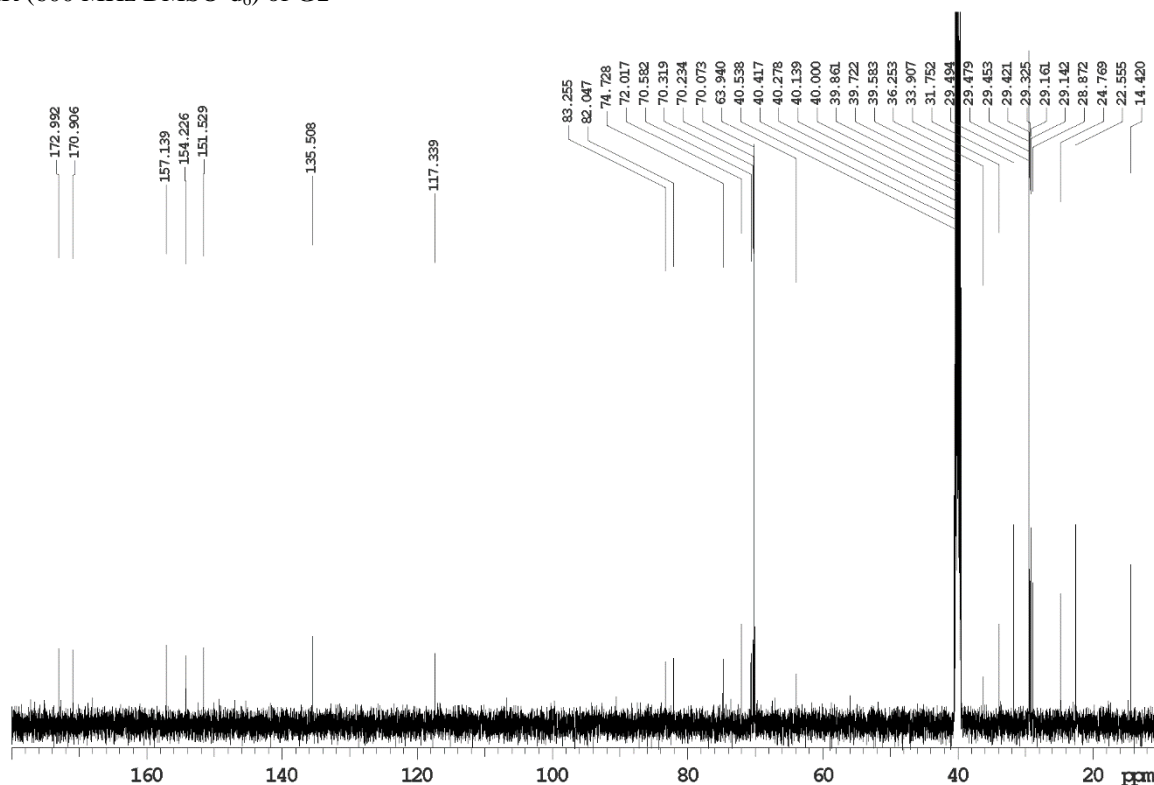
H-NMR (200 MHz DMSO-d<sub>6</sub>) of **4**



H-NMR (600 MHz DMSO-d<sub>6</sub>) of G1



<sup>13</sup>C-NMR (600 MHz DMSO-d<sub>6</sub>) of G1



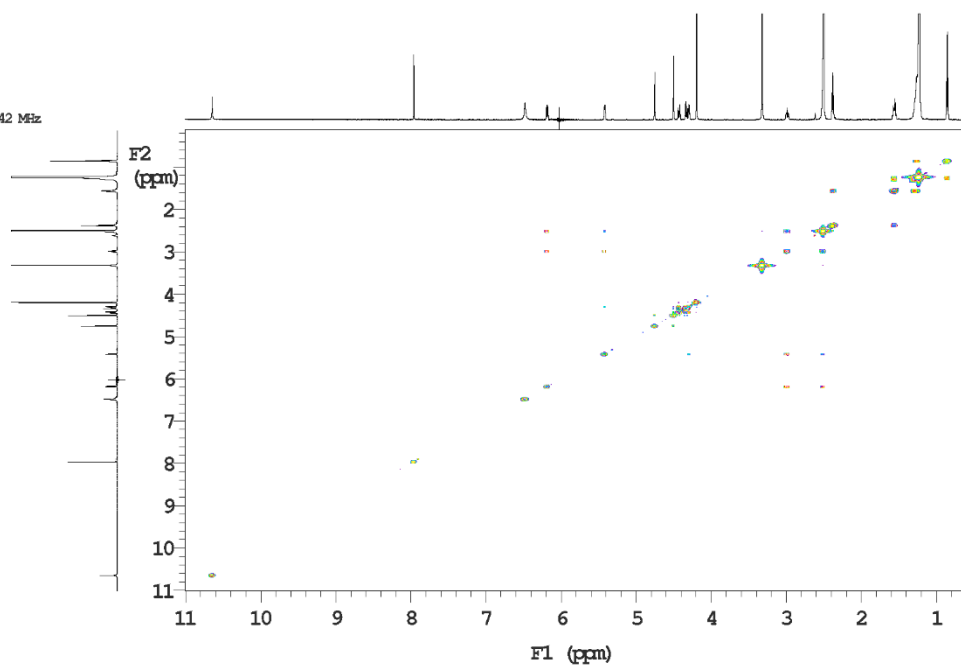
## COSY spectrum (600 MHz DMSO-d<sub>6</sub>) of G1

i600 std parameters

File: dG\_3C18\_5Fc\_H\_8mg\_06ml\_gcosy\_dmsd\_170914

Temp. 25.0 C / 298.1 K  
Operator: sangiac

Relax. delay 1.000 sec  
Acq. time 0.213 sec  
Width 9611.9 Hz  
2D Width 9611.9 Hz  
4 repetitions  
256 increments  
OBSERVE HL, 599.7304242 MHz  
DATA PROCESSING  
Sine bell 0.107 sec  
F1 DATA PROCESSING  
Sine bell 0.027 sec  
FT size 4096 x 4096  
Total time 0 min 0 sec



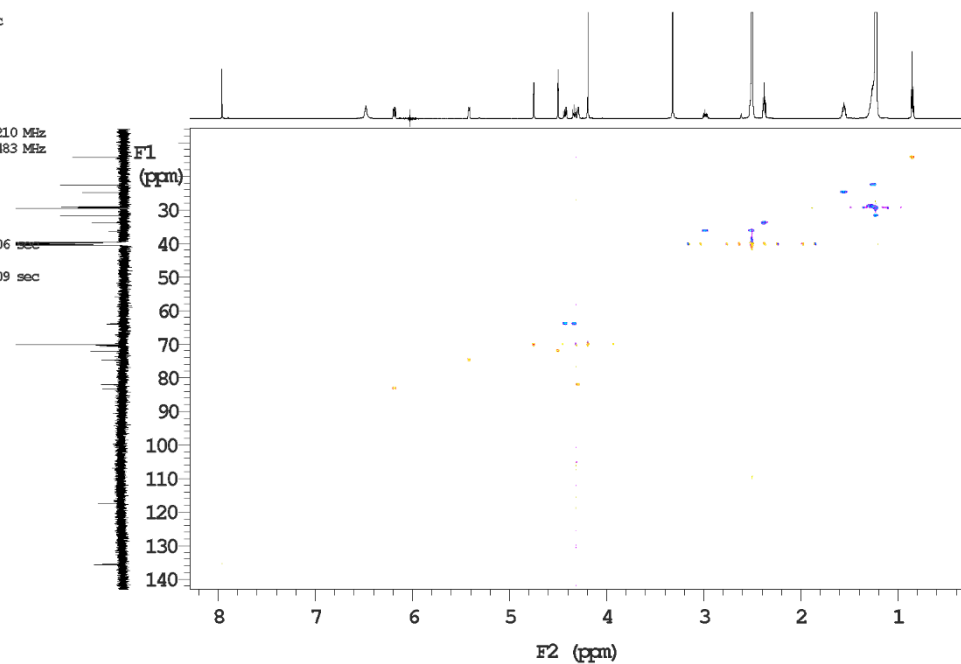
## HSQC spectrum (600 MHz DMSO-d<sub>6</sub>) of G1

i600 std parameters

File: dG\_3C18\_5Fc\_H\_8mg\_06ml\_gHSQCAD\_dmsd\_170914

Temp. 25.0 C / 298.1 K  
Operator: sangiac

Relax. delay 1.000 sec  
Mixing 0.500 sec  
Acq. time 0.230 sec  
Width 9611.9 Hz  
2D Width 25632.8 Hz  
16 repetitions  
2 x 256 increments  
OBSERVE HL, 599.7304210 MHz  
DECOUPLE CL3, 150.8136483 MHz  
Power 43 dB  
on during acquisition  
off during delay  
W40 Triple modulated  
DATA PROCESSING  
Gauss apodization 0.106 sec  
F1 DATA PROCESSING  
Gauss apodization 0.009 sec  
FT size 8192 x 2048  
Total time 0 min 0 sec



# HMBC spectrum (600 MHz DMSO-d<sub>6</sub>) of G1

i600 std parameters

File: dG\_3C18\_5Fc\_H\_8mg\_04nL\_gHMBC\_dmsd\_170914

Temp. 25.0 C / 298.1 K  
Operator: sangiac

Relax. delay 1.000 sec  
Mixing 0.080 sec  
Acq. time 0.128 sec  
Width 9611.9 Hz  
2D Width 36199.1 Hz  
32 repetitions

256 increments  
OBSERVE H1, 599.7304215 MHz

DATA PROCESSING

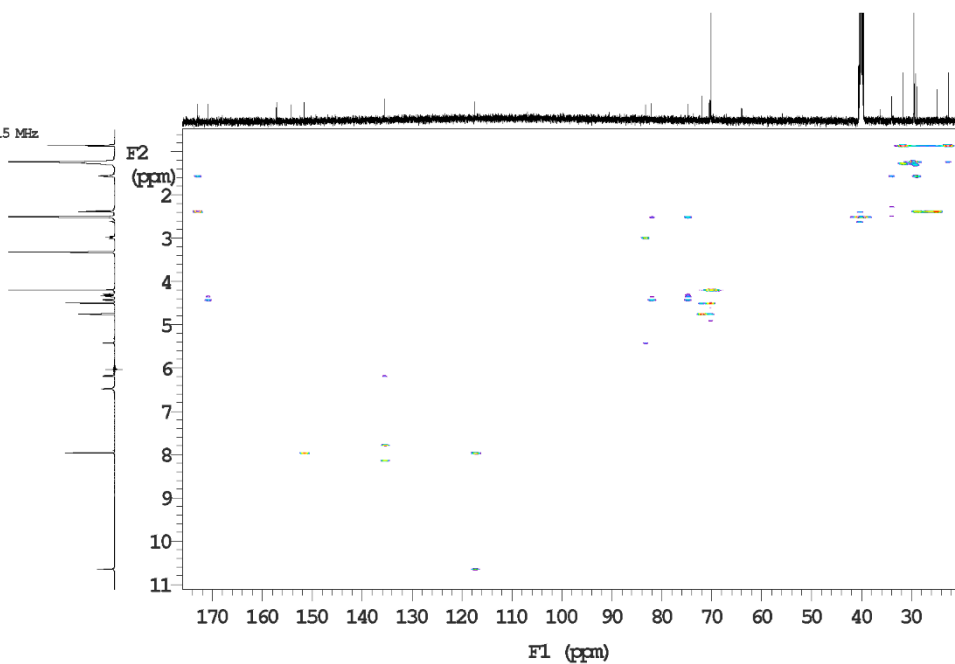
Sine ball 0.064 sec

F1 DATA PROCESSING

Sine ball 0.007 sec

FT size 4096 x 2048

Total time 0 min 0 sec



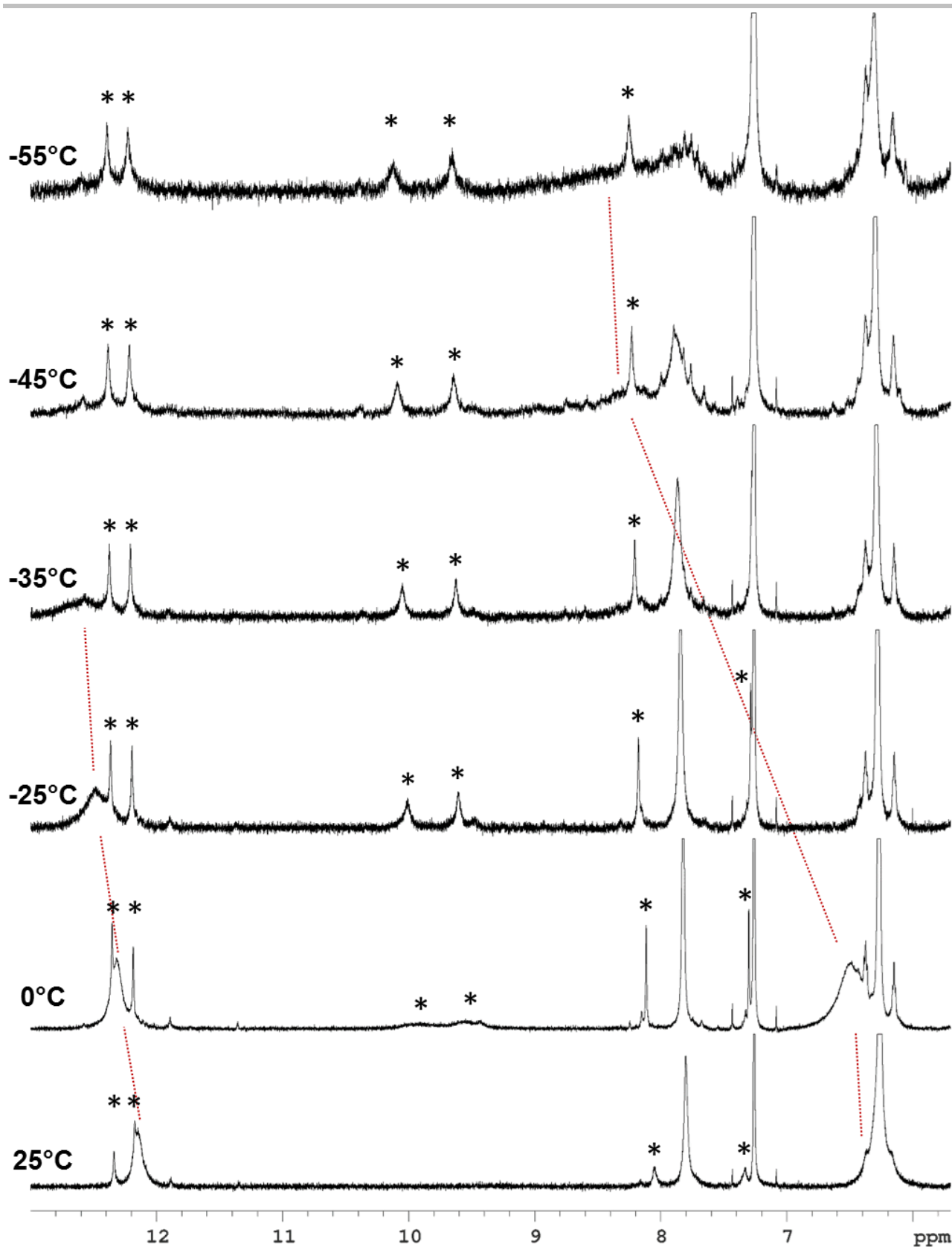


**Figure S1:** downfield portion of the  $^1\text{H}$ -NMR spectrum of **G1** (16 mM) at different temperatures in  $\text{CDCl}_3$ . Guidelines highlight imino and amino N-H shifts. Signals marked with stars belong to the  $\text{C}_4$ -symmetric  $\text{G1}_8\text{K}^+$  complex formed by addition of a small amount of KI to the sample.

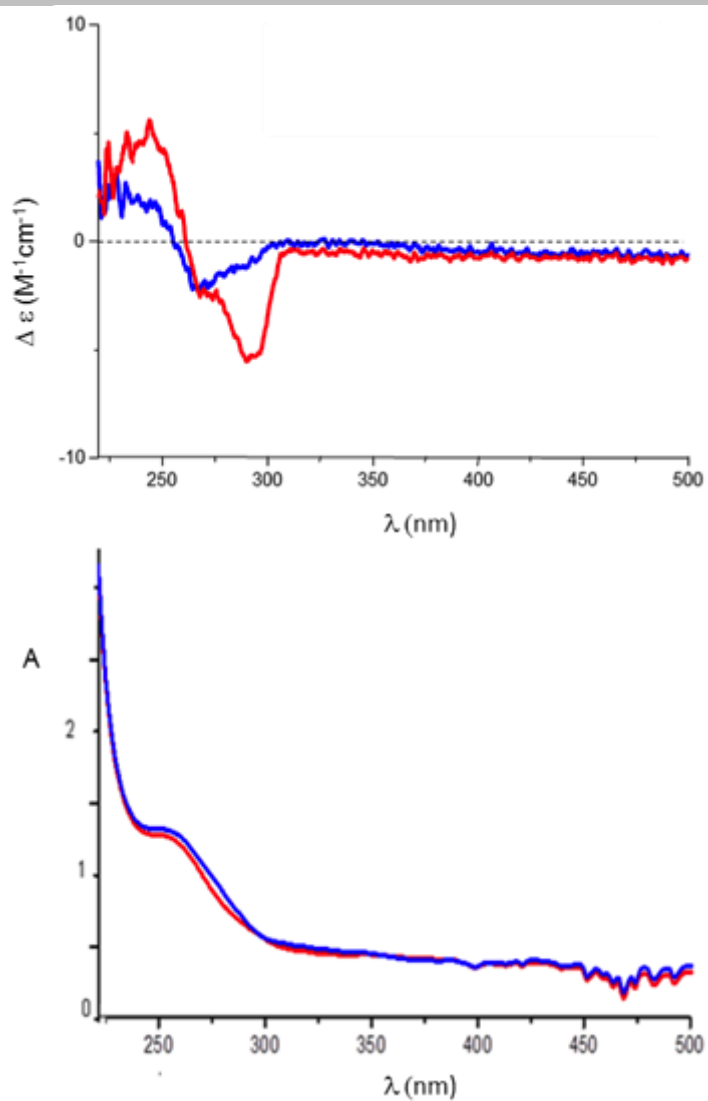
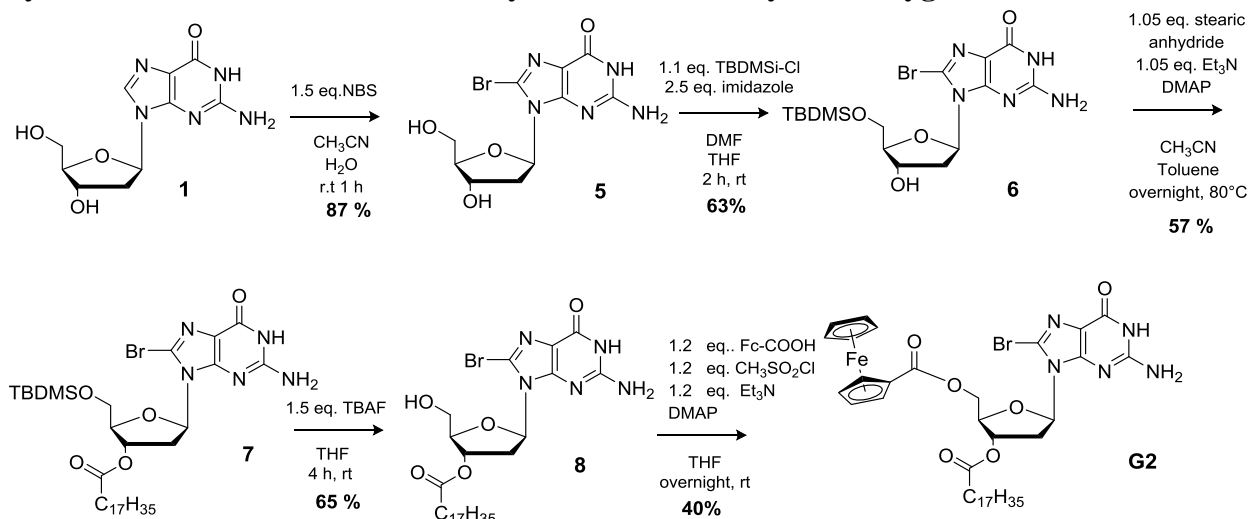


**Figure S2:** CD (top) and UV (bottom) spectra of **G1** (2.5 mM in  $CHCl_3$ ) before (blue) and after (red) addition of potassium picrate (1/8 mol/mol).

## 1.2 Synthesis of 8-bromo-5'-O-ferrocenoyl-3'-O-octadecanoyl-2'-deoxyguanosine G2



### 8-bromo-5'-O-*tert*-butyldimethylsilyl-2'-deoxyguanosine 6

8-Bromo-2'-deoxyguanosine **5**<sup>2</sup> (740 mg, 2.14 mmol) and imidazole (326 mg, 5.35 mmol) were suspended in dry DMF (10 mL) and treated with a solution of *tert*-butyldimethylsilyl chloride (355 mg, 2.35 mmol) in THF (5 mL). The reaction mixture was stirred for 2 h at room temperature, concentrated, diluted in water (20 mL) and extracted with DCM (2 x 20 mL). The organic layer was dried over MgSO<sub>4</sub>, concentrated and purified by chromatography on silica gel (CH<sub>2</sub>Cl<sub>2</sub>: MeOH 93:7) to provide 621 mg (1.35 mmol, 63%) of the title compound as a white powder.

ESI-MS (positive mode, MeOH solution, *m/z*): 461.4 [M+H]<sup>+</sup>, 483.4 [M+Na]<sup>+</sup>.

IR (KBr): 3460, 3321, 3133, 1260 cm<sup>-1</sup>.

<sup>1</sup>H-NMR δ (dms<sub>o</sub>-d<sub>6</sub>): -0.044 and -0.035 (s,s, 6H, SiMe<sub>2</sub>), 0.815 (s, 9H, tBuSi), 2.142 (m, 1H, H<sup>2'</sup>), 3.239 (m, 1H, H<sup>2'</sup>), 3.692 (m, *J*=13.8, *J*=8.4, 1H, H<sup>5'</sup>), 3.768 (m, 2H, H<sup>4'</sup>, H<sup>5'</sup>), 4.427 (m, 1H, H<sup>3'</sup>), 5.245 (d, *J*=4.2, 1H, OH), 6.152 (t, *J*=7.2, 1H, H<sup>1'</sup>), 6.540 (bs, 2H, NH<sub>2</sub>), 10.807 (s, 1H, NH) ppm.

### 8-bromo-5'-O-*tert*-butyldimethylsilyl-3'-O-octadecanoyl-2'-deoxyguanosine 7

Stearic anhydride (780 mg, 1.42 mmol) and a catalytic amount of DMAP were added to a flask containing a suspension of 8-bromo-5'-O-*tert*-butyldimethylsilyl-2'-deoxyguanosine (621 mg, 1.35 mmol, dried in P<sub>2</sub>O<sub>5</sub> *in vacuo* for 2 h at 60°C) in 20 mL of an acetonitrile-toluene 1:1 mixture and TEA (206 μL, 1.42 mmol). The reaction was stirred at 80°C under argon for 12 h. The solvents were removed under reduced pressure and the crude material was dissolved in dichloromethane and extracted three times with sat. NaHCO<sub>3</sub>. The organic layer was then dried over MgSO<sub>4</sub>. The crude material was

<sup>2</sup> L.C.J. Gillet, O. D. Scharer, *Org. Lett.* 2002, **4**, 4205-4208.

---

purified by column chromatography on silica gel using DCM/ methanol (95:5) as eluent affording the desired product as a white solid (560 mg, 0.77 mmol, yield 57%).

ESI-MS (positive mode, MeOH solution,  $m/z$ ): 727.8  $[M+H]^+$ , 749.8  $[M+Na]^+$ .

IR (KBr): 3426, 3310, 3173, 2925, 2880, 1730, 1251  $\text{cm}^{-1}$ .

$^1\text{H-NMR}$   $\delta$ (dms $\text{-d}_6$ ): -0.061 and -0.057 (s,s, 6H, SiMe $_2$ ), 0.799 (s, 9H, tBuSi), 0.848 (t,  $J=7.2$ , 3H, Me), 1.227 (m, 28H, -CH $_2$ -), 1.539 (qi,  $J=7.2$ , 2H, -CO-CH $_2$ -CH $_2$ -), 2.339 (t,  $J=7.2$ , m, 3H, -CO-CH $_2$ - and H $^{2'}$ ), 3.578 (m, 1H, H $^{2'}$ ), 3.796 (m, 2H, H $^{5'}$ ), 3.980 (m, 1H, H $^{4'}$ ), 5.372 (m, 1H, H $^{3'}$ ), 6.158 (t,  $J=7.2$ , 1H, H $^{1'}$ ), 6.524 (bs, 2H, NH $_2$ ), 10.819 (s, 1H, NH) ppm.

### 8-bromo-3'-O-octadecanoyl-2'-deoxyguanosine **8**

Tetrabutylammonium fluoride trihydrate (560 mg, 0,77mmol) was added to a solution of 8-bromo-5'-O-tert-butyltrimethylsilyl-3'-O-octadecanoyl-deoxyguanosine (364 mg, 1.15 mmol) in THF (15 mL) and the solution was stirred for 4 h at room temperature. The solvent was removed under reduced pressure and the crude material was dissolved in dichloromethane and extracted three times with water. The organic layer was then dried over MgSO $_4$ . The crude material was purified by column chromatography on silica gel using dichloromethane /methanol (96:4) as eluent, affording product **8** as a white solid (306 mg, 0.5 mmol, yield 65%)

ESI-MS (positive mode, MeOH solution,  $m/z$ ): 613.6  $[M+H]^+$ , 635.6  $[M+Na]^+$ .

IR (KBr): 3408, 3325, 3156, 2928, 2875, 1730  $\text{cm}^{-1}$ .

$^1\text{H-NMR}$   $\delta$ (dms $\text{-d}_6$ ): 0.851 (t,  $J=6.8$ , 3H, Me), 1.227 (m, 28H, -CH $_2$ -), 1.543 (qi,  $J=6.8$ , 2H, -CO-CH $_2$ -CH $_2$ -), 2.300 (m, 1H, H $^{2'}$ ), 2.352 (t,  $J=7.2$ , 2H, -CO-CH $_2$ -), 3.495 (m, 1H, H $^{2'}$ ), 3.578 (m, 1H, H $^{5'}$ ), 3.651 (m, 1H, H $^{5'}$ ), 3.993 (m, 1H, H $^{4'}$ ), 4.956 (t,  $J=5.5$ , 1H, OH), 5.347 (m, 1H, H $^{3'}$ ), 6.123 (t,  $J=7.2$ , 1H, H $^{1'}$ ), 6.507 (bs, 2H, NH $_2$ ), 10.833 (s, 1H, NH) ppm.

### 8 bromo-5'-O-ferrocenoyl-3'-O-octadecanoyl-2'-deoxyguanosine **G2**

Ferrocene carboxylic acid (138 mg, 0.6 mmol) and 8-bromo-3'-O-decanoyl-2'-deoxyguanosine (306 mg, 0.5 mmol) were dried over P $_2$ O $_5$  *in vacuo* for 2 h at 60°C. Ferrocene carboxylic acid was dissolved in dry THF (10 mL), Et $_3$ N (79  $\mu\text{L}$ , 0.6 mmol) was added and the resulting solution was cooled at 0° C under argon atmosphere. Methanesulfonyl-chloride (CH $_3$ SO $_2$ Cl 46  $\mu\text{L}$ , 0.6 mmol) was added and the reaction was stirred at the same temperature for two hours. 8-Bromo-3'-O-decanoyl-2'-deoxyguanosine and DMAP (catalytic amount) were then added and the solution was stirred for 12 hours at room temperature. The solvent was removed under reduced pressure, the crude was dissolved in dichloromethane and extracted with sat. NaHCO $_3$ . The organic layer was dried over MgSO $_4$ . The residue was applied to a silica gel column packed in dichloromethane and eluted with a gradient of

---

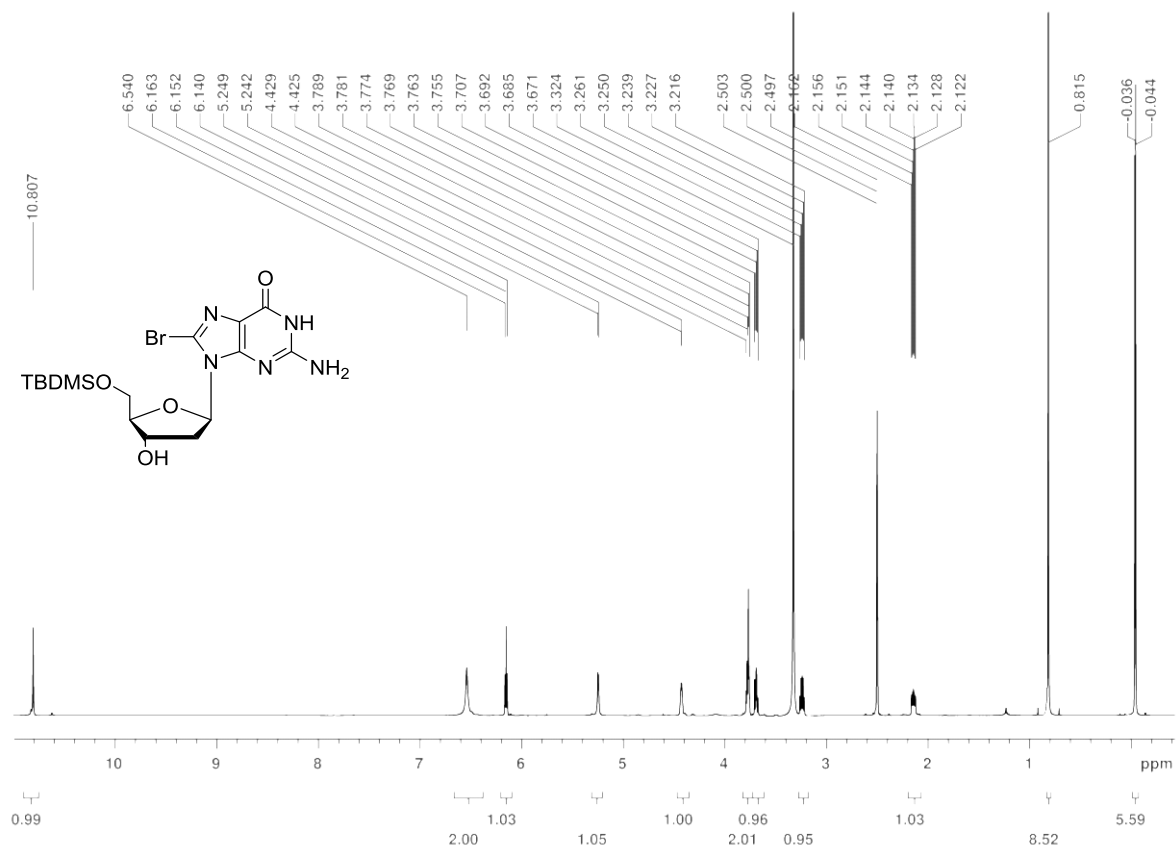
methanol in dichloromethane. The target product was eluted with a mixture of dichloromethane-methanol (97:3) and crystallized from MeOH, yielding **G2** as a yellow solid (165 mg, 0.20 mmol, yield 40%).

ESI-MS (positive mode, MeOH solution,  $m/z$ ): 825.6  $[M+H]^+$ , 847.6  $[M+Na]^+$ .

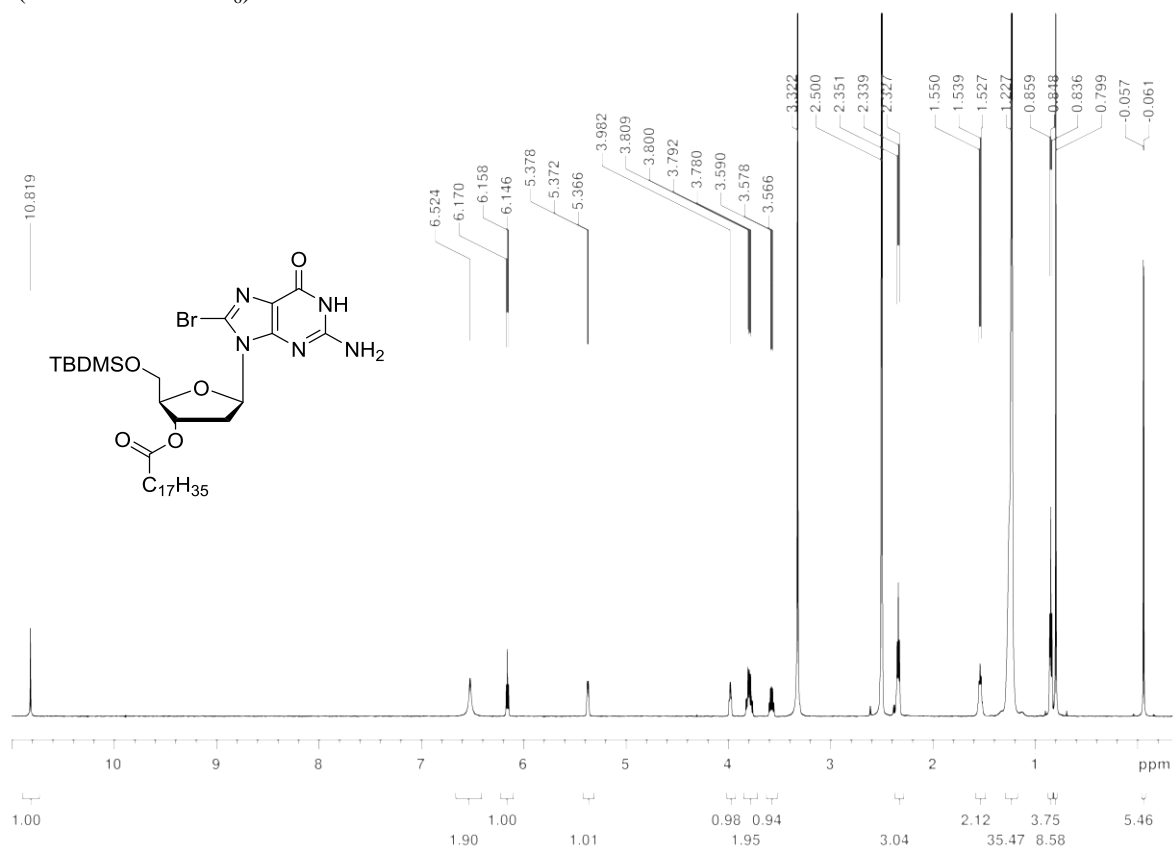
IR (KBr): 3340 3196, 2961, 2877, 1732, 1679, 481  $\text{cm}^{-1}$ .

$^1\text{H-NMR}$   $\delta$  (dms $\text{-d}_6$ ): 0.850 (t,  $J=7.2$ , 3H, Me)-CH $_2$ -), 1.556 (qi,  $J=7.2$ , 2H, -CO-CH $_2$ -CH $_2$ -), 2.377 (t,  $J=7.2$ , 2H, -CO-CH $_2$ -), 2.458 (m, 1H, H $^{2'}$ ), 3.609 (m, 1H, H $^{2'}$ ), 4.144 (s, 5H, Fc\_C $_5$ H $_5$ ), 4.288 (m, 1H, H $^{4'}$ ), 4.435 (m, 2H, H $^{5'}$ ), 4.465 (t,  $J=1.9$ , 2H, C $_5$ H $_4$ -Fc), 4.714 (t,  $J=1.9$ , 2H, C $_5$ H $_4$ -Fc), 5.532 (m, 1H, H $^{3'}$ ), 6.223 (m, 1H, H $^{1'}$ ), 6.554 (bs, 2H, NH $_2$ ), 10.876 (s, 1H, NH) ppm.  $^{13}\text{C-NMR}$   $\delta$  (dms $\text{-d}_6$ ): 14.420 (Me), 22.552 (CH $_2$ ), 24.791(-CO-CH $_2$ -), 28.850 (CH $_2$ ), 29.157 (CH $_2$ ), 29.311 (CH $_2$ ), 29.472 (CH $_2$ ), 31.748 (CH $_2$ ), 33.896 (-CO-CH $_2$ -CH $_2$ -), 34.046 (C $^{2'}$ ), 63.863 (C $^{5'}$ ), 69.818 (Fc\_C $_5$ H $_5$ ), 70.048 (Fc\_C $_5$ H $_4$ ), 70.701 (Fc C $^{IV}$ -CO), 71.925 (Fc\_C $_5$ H $_4$ ), 74.853 (C $^{3'}$ ), 82.314 (C $^{4'}$ ), 85.831 (C $^{1'}$ ), 117.968 (C $_5$ ), 121.181 (C $_8$ ), 152.452 (C $_4$ ), 153.934, 155.943, 170.844 (CO-Fc), 173.058 (CO-CH $_2$ ) ppm.

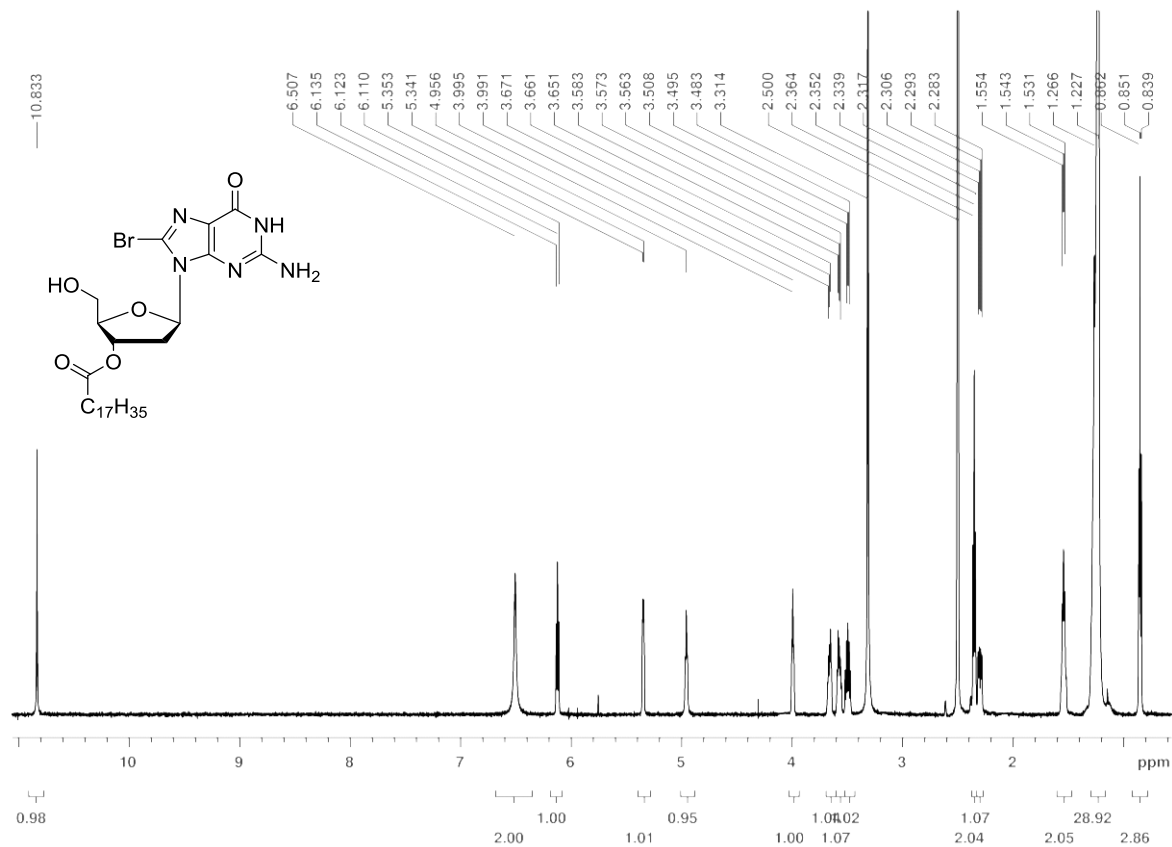
H-NMR (200 MHz DMSO-d<sub>6</sub>) of **6**



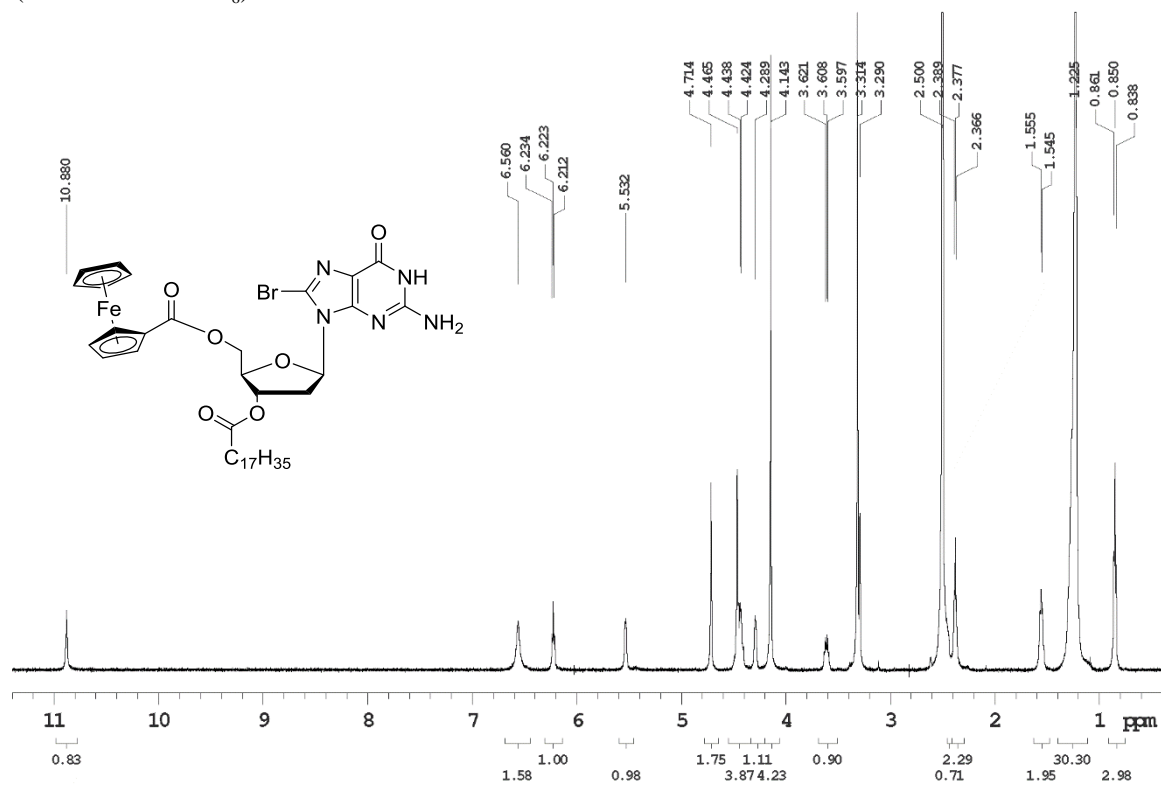
H-NMR (200 MHz DMSO-d<sub>6</sub>) of **7**



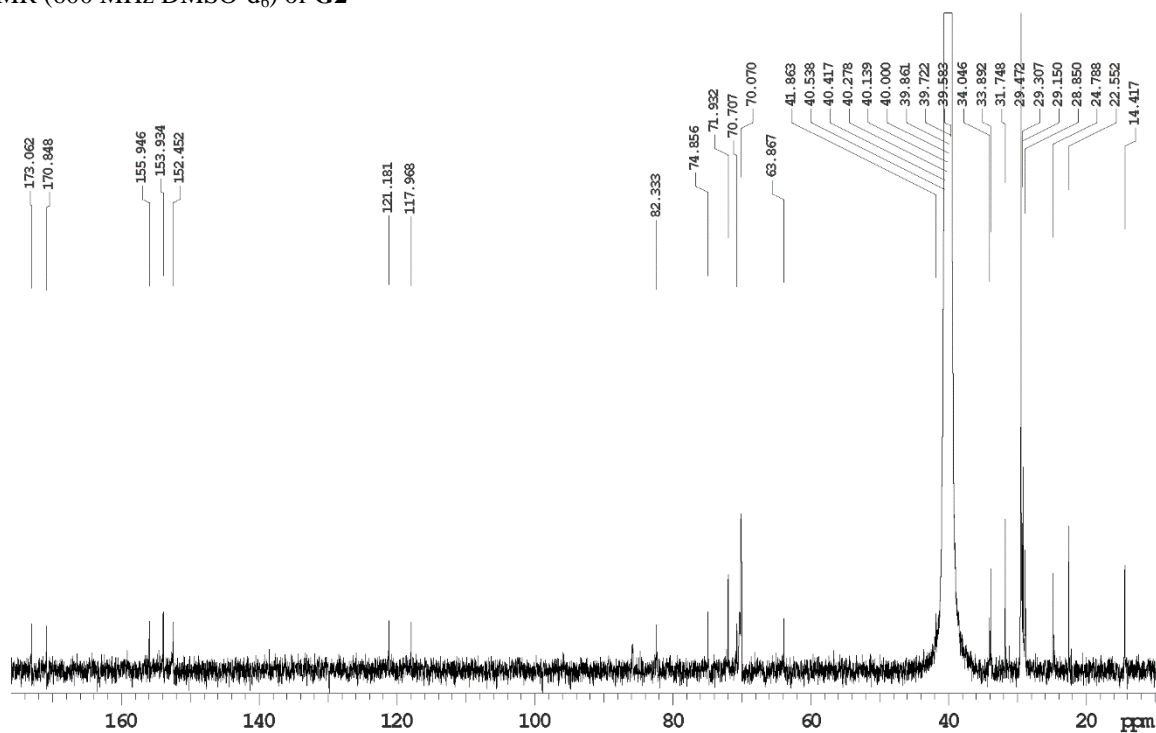
H-NMR (200 MHz DMSO-d<sub>6</sub>) of **8**



H-NMR (600 MHz DMSO-d<sub>6</sub>) of **G2**



C13 -NMR (600 MHz DMSO-d<sub>6</sub>) of G2



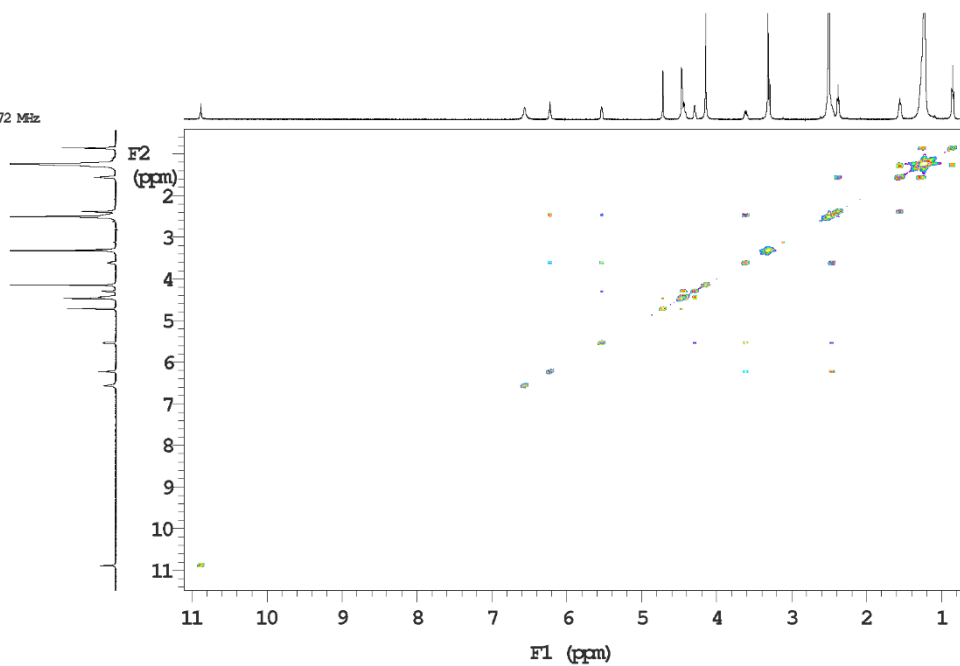
COSY-NMR (600 MHz DMSO-d<sub>6</sub>) of G2

i600 std parameters

File: dG\_8Br\_3Cl8\_5Fc\_gCOSY\_dmsd\_190314

Temp. 25.0 C / 298.1 K  
Operator: sangiac

Relax. delay 1.000 sec  
Acq. time 0.213 sec  
Width 9611.9 Hz  
2D Width 9611.9 Hz  
8 repetitions  
256 increments  
OBSERVE H1, 599.7304272 MHz  
DATA PROCESSING  
Sine ball 0.107 sec  
F1 DATA PROCESSING  
Sine ball 0.027 sec  
FT size 4096 x 4096  
Total time 0 min 0 sec



## HSQC-NMR (600 MHz DMSO-d<sub>6</sub>) of G2

i600 std parameters

File: dG\_8Br\_3Cl18\_5Fc\_gHSQCad\_dms0\_190314

Temp. 25.0 C / 298.1 K  
Operator: sangiac

Relax. delay 1.000 sec  
Mixing 0.500 sec  
Acq. time 0.230 sec  
Width 9611.9 Hz  
2D Width 25632.8 Hz  
16 repetitions  
2 x 256 increments

OBSERVE H1, 599.7304205 MHz  
DECOUPLE CL3, 150.8136483 MHz

Power 43 dB  
on during acquisition  
off during delay  
WFO Triple modulated

DATA PROCESSING

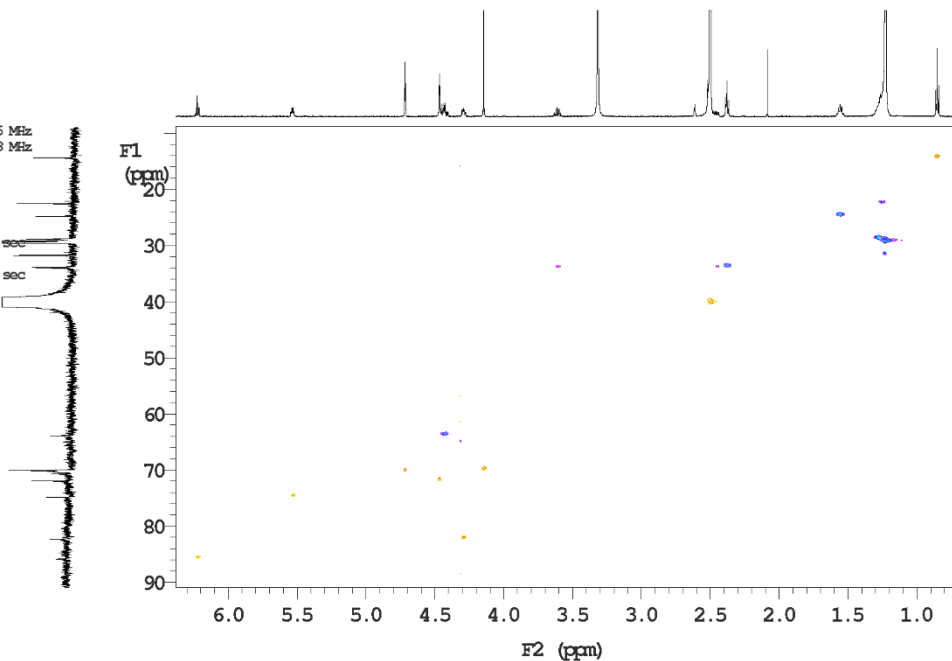
Gauss apodization 0.106 sec

F1 DATA PROCESSING

Gauss apodization 0.009 sec

FT size 8192 x 2048

Total time 0 min 0 sec



## HMBC-NMR (600 MHz DMSO-d<sub>6</sub>) of G2

i600 std parameters

File: dG\_8Br\_3Cl18\_5Fc\_gHMBC\_dms0\_190314

Temp. 25.0 C / 298.1 K  
Operator: sangiac

Relax. delay 1.000 sec  
Mixing 0.080 sec  
Acq. time 0.128 sec  
Width 9611.9 Hz  
2D Width 36199.1 Hz  
64 repetitions  
256 increments

OBSERVE H1, 599.7304224 MHz

DATA PROCESSING

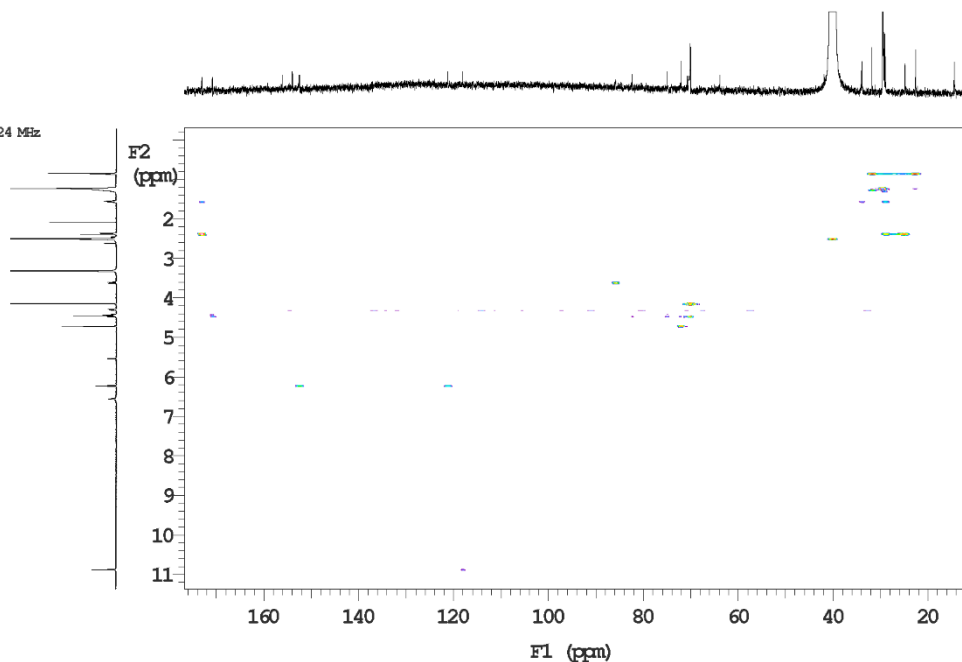
Sine ball 0.064 sec

F1 DATA PROCESSING

Sine ball 0.007 sec

FT size 4096 x 2048

Total time 0 min 0 sec



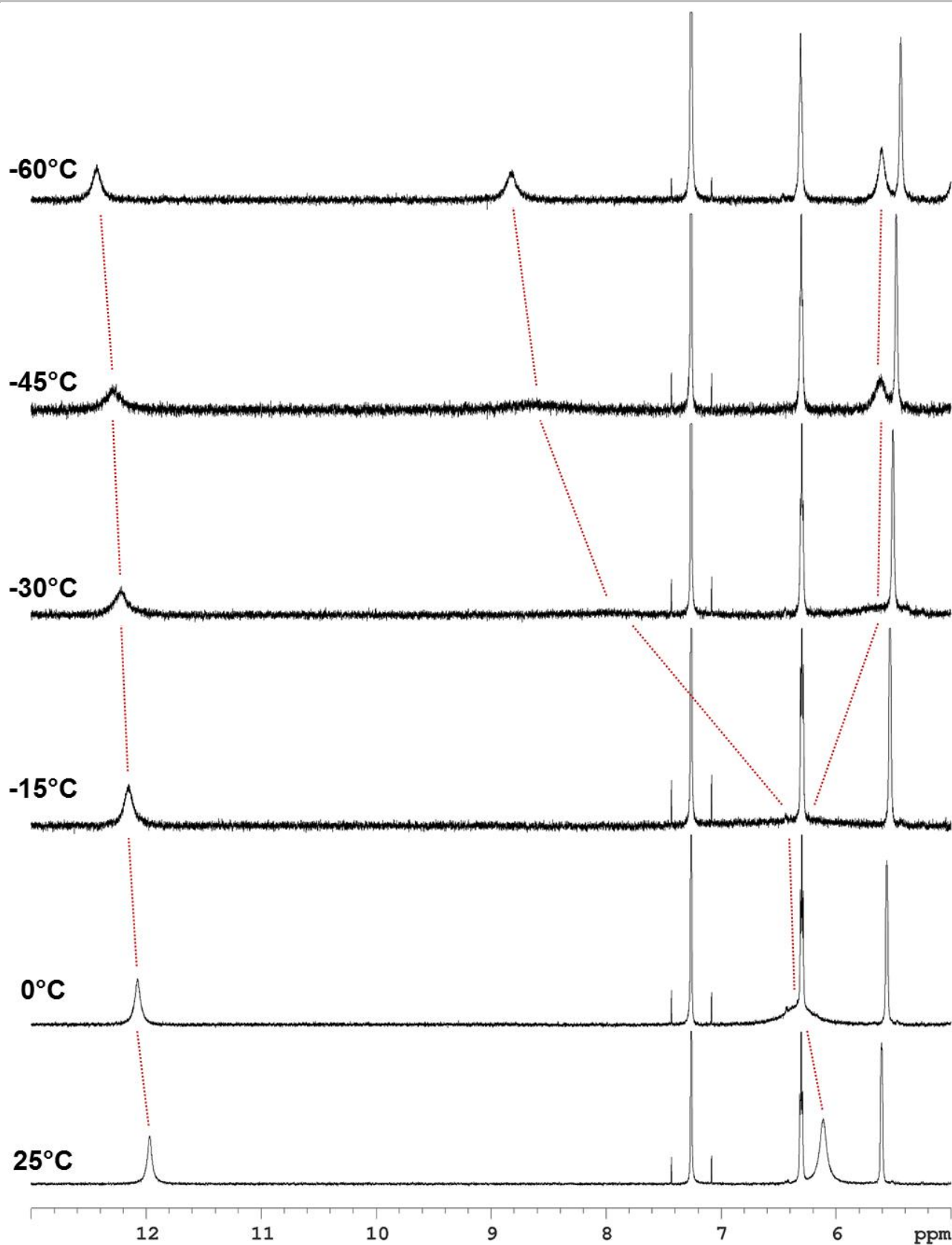


**Figure S3:** downfield portion of the  $^1\text{H-NMR}$  spectrum of G2 (9 mM) at different temperatures in  $\text{CDCl}_3$ . Guidelines highlight imino and amino N-H shifts.

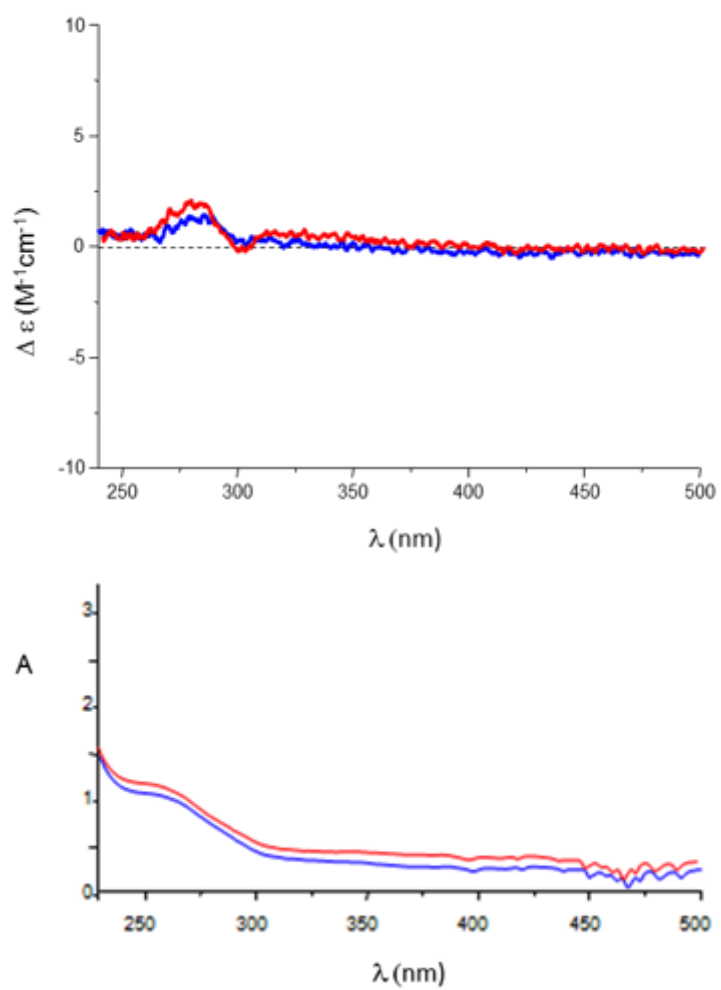
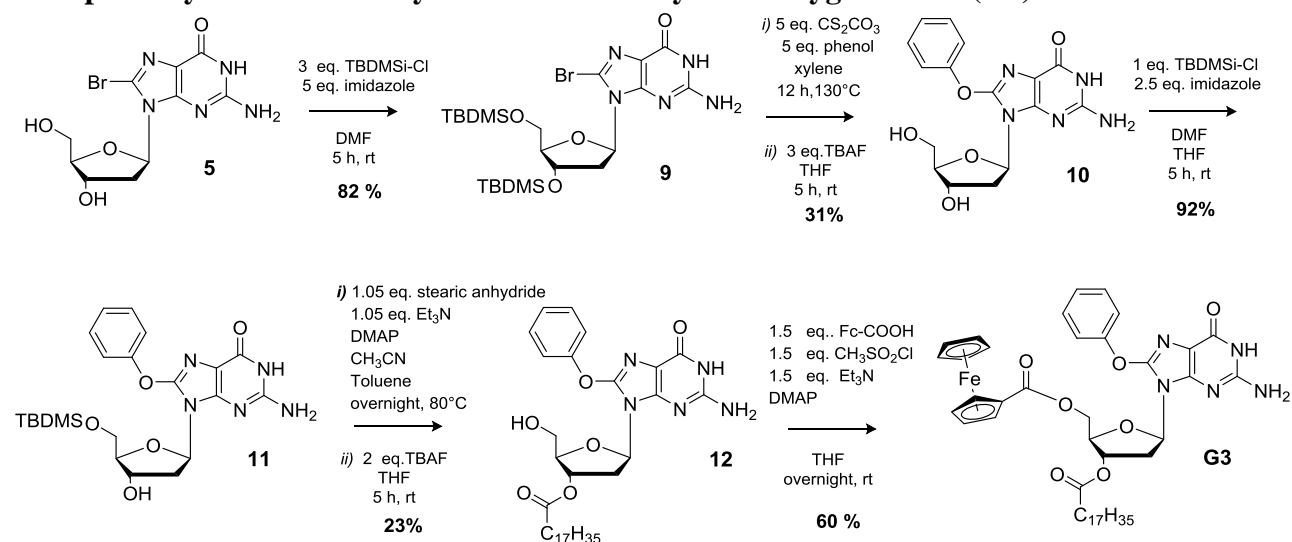


**Figure S4:** CD (top) and UV (bottom) spectra of **G2** (2.5 mM in  $CHCl_3$ ) before (blue) and after (red) addition of potassium picrate (1/8 mol/mol).

### 1.3 8-phenoxy-5'-*O*-ferrocenoyl-3'-*O*-octadecanoyl-2'-deoxyguanosine (G3)



#### 8-bromo-3'-5'-*O*-bis-(*tert*-butyldimethylsilyl)-2'-deoxyguanosine **9**

8-bromo-2'-deoxyguanosine **5** (266 mg, 0.74 mmol) and imidazole (1.09 g, 16 mmol) were suspended in dry DMF (20 mL). *t*-butyldimethylsilyl chloride (1.45 g, 9.6 mmol) was added and the reaction mixture was stirred for 5h at room temperature, concentrated, diluted in water (20 mL) and extracted with EtOAc (3 x 20 mL). The organic layer was dried over MgSO<sub>4</sub> and concentrated to provide 1.52 g (1.35 mmol, 82%) of the title compound as a white powder.

ESI-MS (positive mode, MeOH solution,  $m/z$ ): 575.9 [M+H]<sup>+</sup>, 597.9 [M+Na]<sup>+</sup>.

IR (KBr): 3423, 3306, 3188, 1249, 1015 cm<sup>-1</sup>

<sup>1</sup>H-NMR  $\delta$ (dms<sub>o</sub>-d<sub>6</sub>): -0.020 and -0.005 (s,s, 6H, SiMe<sub>2</sub>), 0.114 (s, 6H, SiMe<sub>2</sub>), 0.830 (s, 9H, tBuSi), 0.894 (s, 9H, tBuSi), 2.158 (m, 1H, H<sup>2'</sup>), 3.401 (m, 1H, H<sup>2''</sup>), 3.670 (m, 1H), 3.775 (m, 2H), 4.582 (m, 1H), 6.143 (t,  $J=7$ , 1H, H<sup>1'</sup>), 6.406 (bs, 2H, NH<sub>2</sub>), 10.806 (s, 1H, NH) ppm.

#### 8-Phenoxy-2'-deoxyguanosine **10**

To a suspension of Cs<sub>2</sub>CO<sub>3</sub> (4.32 g, 13.2 mmol) in dry xylene was added phenol (1.24 g 13.2 mmol) and the mixture was heated at 130° C for 1 h. 8-Bromo-3'-5'-*O*-bis-(*tert*-butyldimethylsilyl)-2'-deoxyguanosine (1.52 g, 2.65 mmol) was then added and the reaction mixture was stirred at the same temperature for 12 h. The solvent was removed under reduced pressure, the crude was dissolved in ethyl acetate and extracted with a sat. NaHCO<sub>3</sub>. The organic layer was dried over MgSO<sub>4</sub>. The residue was applied to a silica gel column and eluted with dichloromethane/methanol (98:2). 8-Phenoxy-3'-5'-*O*-bis-(*tert*-butyldimethylsilyl)-2'-deoxyguanosine was isolated as a white solid (500 mg, 0,85 mmol, 32 %).

ESI-MS (positive mode, MeOH solution,  $m/z$ ): 588.1 [M+H]<sup>+</sup>, 610.1 [M+Na]<sup>+</sup>

---

<sup>1</sup>H-NMR  $\delta$ (dms<sub>o</sub>-d<sub>6</sub>): -0.066 and -0.055 (s,s, 6H, SiMe<sub>2</sub>), 0.070 (s, 6H, SiMe<sub>2</sub>), 0.795 (s, 9H, tBuSi), 0.872 (s, 9H, tBuSi), 2.180 (m, 1H, H<sup>2'</sup>), 3.002 (m, 1H, H<sup>2'</sup>), 3.570 (m, 2H), 3.764 (m, 1H), 4.494 (m, 1H, H<sup>3'</sup>), 6.207 (t, *J*=7, 1H, H<sup>1'</sup>), 6.421 (bs, 2H, NH<sub>2</sub>), 7.253 (m, 3H, ArH), 7.447 (m, 2H, ArH), 10.682 (s, 1H, NH) ppm.

Tetrabutylammonium fluoride trihydrate (804 mg, 2.55 mmol) was added to a solution of 8-phenoxy-3'-5'-*O*-bis-(*tert*-butyldimethylsilyl)-2'-deoxyguanosine (500 mg, 0.85 mmol) in THF (15 mL) and the solution was stirred for 4 h at room temperature. The solvent was removed under reduced pressure and the crude material was dissolved in dichloromethane and extracted three times with water. The organic layer was then dried over MgSO<sub>4</sub>. The crude material was purified by column chromatography on silica gel using dichloromethane /methanol (85:15) as eluent, affording 8-phenoxy-2'-deoxyguanosine **10** as a white solid (290 mg, 0.81 mmol, yield 95 %).

ESI-MS (positive mode, MeOH solution, *m/z*): 359.9 [M+H]<sup>+</sup>

IR (KBr): 3406, 3320, 3182, 3101, 3066, 1167 cm<sup>-1</sup>

<sup>1</sup>H-NMR  $\delta$ (dms<sub>o</sub>-d<sub>6</sub>): 2.156 (m, 1H, H<sup>2'</sup>), 2.914 (m, 1H, H<sup>2'</sup>), 3.467 (m, 2H), 3.766 (m, 1H), 4.330 (m, 1H, H<sup>3'</sup>), 4.819 (t, *J*=5.6, 1H, OH<sup>5'</sup>), 5.240 (d, *J*=3.2, 1H, OH<sup>3'</sup>), 6.207 (t, *J*=7.2, 1H, H<sup>1'</sup>), 6.416 (bs, 2H, NH<sub>2</sub>), 7.291 (m, 3H, ArH), 7.452 (m, 2H, ArH), 10.626 (s, 1H, NH) ppm.

Elemental analysis calcd (%) for C<sub>16</sub>H<sub>17</sub>N<sub>5</sub>O<sub>5</sub>: C 53.48, H 4.77, N 19.49; found: C 53.56, H 4.76, N 19.51.

### 8-phenoxy-5'-*O*-(*tert*-butyldimethylsilyl)-2'-deoxyguanosine **11**

8-phenoxy-2'-deoxyguanosine (266 mg, 0.74 mmol) and imidazole (126 mg, 1.85 mmol) were suspended in dry DMF (10 mL) and treated with a solution of *tert*-butyldimethylsilyl chloride (112 mg, 0.74 mmol) in THF (2 mL). The reaction mixture was stirred for 2 h at room temperature, concentrated, dissolved in DCM (2 x 20 mL) and extracted with sat. NaHCO<sub>3</sub>. The organic layer was dried over MgSO<sub>4</sub>, concentrated and purified by chromatography on silica gel (CH<sub>2</sub>Cl<sub>2</sub>:MeOH 9:1) to provide 320 mg (0.68 mmol, 92 %) of the title compound as a white powder.

ESI-MS (positive mode, MeOH solution, *m/z*): 474.1 [M+H]<sup>+</sup>

IR (KBr): 3412, 3317, 3103, 3040, 1249, 1167 cm<sup>-1</sup>

<sup>1</sup>H-NMR  $\delta$ (dms<sub>o</sub>-d<sub>6</sub>): -0.064 (s, 6H, SiMe<sub>2</sub>), 0.793 (s, 9H, tBuSi), 2.163 (m, 1H, H<sup>2'</sup>), 2.930 (m, 1H, H<sup>2'</sup>), 3.606 (m, 2H), 3.762 (m, 1H), 4.319 (m, 1H, H<sup>3'</sup>), 5.280 (d, *J*=4.0, 1H, OH), 6.211 (t, *J*=7.0, 1H, H<sup>1'</sup>), 6.428 (bs, 2H, NH<sub>2</sub>), 7.270 (m, 3H, ArH), 7.43 (m, 2H, ArH), 10.615 (s, 1H, NH) ppm.

### 8-phenoxy-3'-*O*-octadecanoyl-2'-deoxyguanosine **12**

---

Stearic anhydride (391 mg, 0.71 mmol) and a catalytic amount of DMAP were added to a flask containing a suspension of 8-phenoxy-5'-*O*-(*tert*-butyldimethylsilyl)-2'-deoxyguanosine (320 mg, 0.68 mmol, dried over P<sub>2</sub>O<sub>5</sub> *in vacuo* for 2 h at 60°C) in 20 mL of a 1:1 mixture of acetonitrile and toluene. TEA (102 μL, 0.71 mmol) was added and the reaction mixture was stirred at 80° C under argon for 4 h. Solvents were removed under reduced pressure and the crude material was dissolved in dichloromethane and extracted three times with sat. NaHCO<sub>3</sub>. The organic layer was then dried over MgSO<sub>4</sub>. The crude material was purified by column chromatography on silica gel using dichloromethane/ methanol (97:3) as eluent, affording 8-phenoxy-5'-*O*-(*tert*-butyldimethylsilyl)-3'-*O*-octadecanoyl-2'-deoxyguanosine as a white solid (240 mg, 0.33 mmol, yield 48%).

ESI-MS (positive mode, MeOH solution, *m/z*): 740.4 [M+H]<sup>+</sup>

<sup>1</sup>H-NMR δ(dms<sub>o</sub>-d<sub>6</sub>): -0.079 (s, 6H, SiMe<sub>2</sub>), 0.775 (s, 9H, tBuSi), 0.837 (t, *J*=7.0, 3H, Me), 1.214 (m, 28H, -CH<sub>2</sub>-), 1.526 (qi, *J*=6.7, 2H, -CO-CH<sub>2</sub>-CH<sub>2</sub>-), 2.322 (m, 3H, H<sup>2'</sup>, -CO-CH<sub>2</sub>-), 3.269 (m, 1H, H<sup>2'</sup>), 3.850 (m, 2H, H<sup>5'</sup>), 3.960 (m, 1H, H<sup>4'</sup>), 5.344 (m, 1H, H<sup>3'</sup>), 6.205 (t, 1H, H<sup>1'</sup>), 6.447 (bs, 2H, NH<sub>2</sub>), 7.287 (m, 3H, ArH), 7.443 (m, 2H, ArH), 10.652 (s, 1H, NH) ppm.

Elemental analysis calcd (%) for C<sub>40</sub>H<sub>65</sub>N<sub>5</sub>O<sub>6</sub>Si: C 64.92, H 8.85, N 9.46; found: C 64.87, H 8.84, N 9.47.

Tetrabutylammonium fluoride trihydrate (170 mg, 0.54 mmol) was added to a solution of 8-phenoxy-5'-*O*-(*tert*-butyldimethylsilyl)-3'-*O*-octadecanoyl-2'-deoxyguanosine (200 mg, 0.27 mmol) in THF (5 mL) and the solution was stirred for 3 h at room temperature. The solvent was removed under reduced pressure and the crude material was dissolved in dichloromethane and extracted three times with water. The organic layer was then dried over MgSO<sub>4</sub>. The crude material was purified by column chromatography on silica gel using dichloromethane /methanol (96:4) as eluent, affording 8-phenoxy-3'-*O*-octadecanoyl-2'-deoxyguanosine **12** as a white solid (100 mg, 0.16 mmol, yield 30 %)

ESI-MS (positive mode, MeOH solution, *m/z*): 626.4 [M+H]<sup>+</sup>, 648.3 [M+Na]<sup>+</sup>.

IR (KBr): 3327, 3142, 3030, 2928, 2875, 1725, 1160 cm<sup>-1</sup>.

<sup>1</sup>H-NMR δ(dms<sub>o</sub>-d<sub>6</sub>): 0.846 (t, *J*=6.6, 3H, Me), 1.220 (m, 28H, -CH<sub>2</sub>-), 1.527 (qi, *J*=6.6, 2H, -CO-CH<sub>2</sub>-CH<sub>2</sub>-), 2.337 (m, 3H, H<sup>2'</sup>, -CO-CH<sub>2</sub>-), 3.234 (m, 1H, H<sup>2'</sup>), 3.547 (m, 2H, H<sup>5'</sup>), 3.960 (m, 1H, H<sup>4'</sup>), 4.965 (t, *J*=5.6, 1H, OH), 5.328 (m, 1H, H<sup>3'</sup>), 6.179 (t, *J*=7.0, 1H, H<sup>1'</sup>), 6.427 (bs, 2H, NH<sub>2</sub>), 7.319 (m, 3H, ArH), 7.454 (m, 2H, ArH), 10.654 (s, 1H, NH) ppm.

### 8-phenoxy-5'-*O*-ferrocenoyl-3'-*O*-octadecanoyl-2'-deoxyguanosine **G3**

Ferrocene carboxylic acid (55.2 mg, 0.24 mmol) and 8-phenoxy-3'-*O*-decanoyl-2'-deoxyguanosine (100 mg, 0.16 mmol) were dried over P<sub>2</sub>O<sub>5</sub> *in vacuo* for 2 h at 60°C. Ferrocene carboxylic acid was

---

dissolved in dry THF(5 mL), Et<sub>3</sub>N (108 μL, 0.24mmol) was added and the resulting solution was cooled at 0° C. (18 μl, 0.24mmol) was added and stirring was continued at the same temperature for 2 h. 8-Phenoxy-3'-*O*-decanoyl-2'-deoxyguanosine and DMAP (catalytic amount) were then added and the mixture was allowed to reach room temp. After 12 hours, the solvent was removed under reduced pressure, the residue was dissolved in dichloromethane and extracted with sat. NaHCO<sub>3</sub>. The organic layer was dried over MgSO<sub>4</sub> and the crude reaction mixture was applied to a silica gel column packed in dichloromethane and eluted with a gradient of methanol in dichloromethane. The final product was eluted with a mixture of dichloromethane-methanol (98:2) and crystallized in MeOH, affording the title product as a yellow solid (80 mg, 0.095 mmol, yield 60%).

ESI-MS (positive mode, MeOH solution, *m/z*): 838.3 [M+H]<sup>+</sup>, 860.3 [M+Na]<sup>+</sup>.

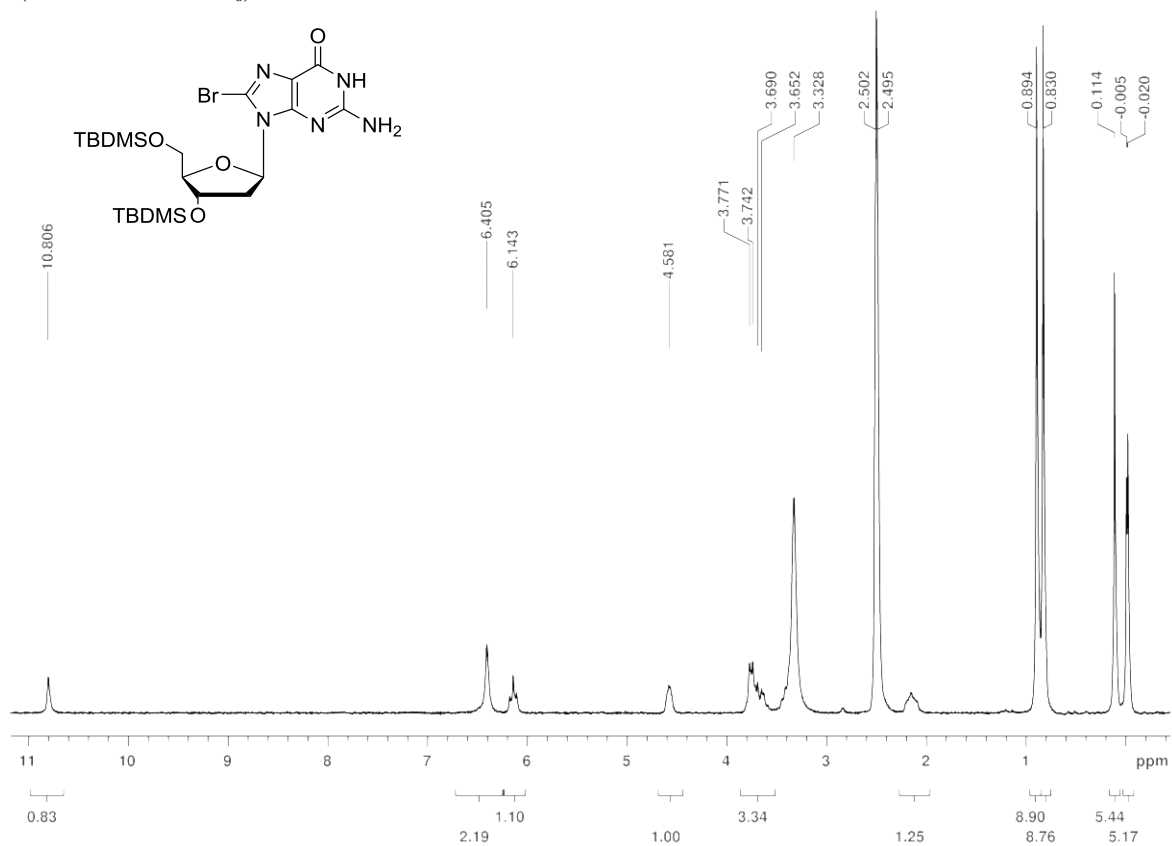
IR (KBr): 3413, 3308, 3157, 3040, 3027, 2937, 2865, 1731, 1679, 1163, 495 cm<sup>-1</sup>.

<sup>1</sup>H-NMR δ(dms<sub>o</sub>-d<sub>6</sub>): 0.846 (t, *J*=7.2, 3H, Me), 1.213 (m, 28H, -CH<sub>2</sub>-), 1.546 (qi, *J*=7.2, 2H, -CO-CH<sub>2</sub>-CH<sub>2</sub>-), 2.366 (t, *J*=7.2, 2H, -CO-CH<sub>2</sub>-), 2.471 (m, 1H, H<sup>2'</sup>), 3.383 (m, 1H, H<sup>2'</sup>), 4.140 (s, 5H, Fc-C<sub>5</sub>H<sub>5</sub>), 4.280 (m, 1H, H<sup>4'</sup>), 4.348 (m, 1H, H<sup>5'</sup>), 4.399 (m, 1H, H<sup>5'</sup>), 4.430 (m, 2H, Fc-C<sub>5</sub>H<sub>4</sub>), 4.698 (m, 2H, Fc-C<sub>5</sub>H<sub>4</sub>), 5.479 (m, 1H, H<sup>3'</sup>), 6.276 (t, *J*=7.2, 1H, H<sup>1'</sup>), 6.467 (bs, 2H, NH<sub>2</sub>), 7.266 (t, *J*=7.2, 1H, ArH), 7.351 (d, *J*=7.2, 2H, ArH), 7.447 (t, *J*=7.2, 2H, ArH), 10.705 (s, 1H, NH) ppm.

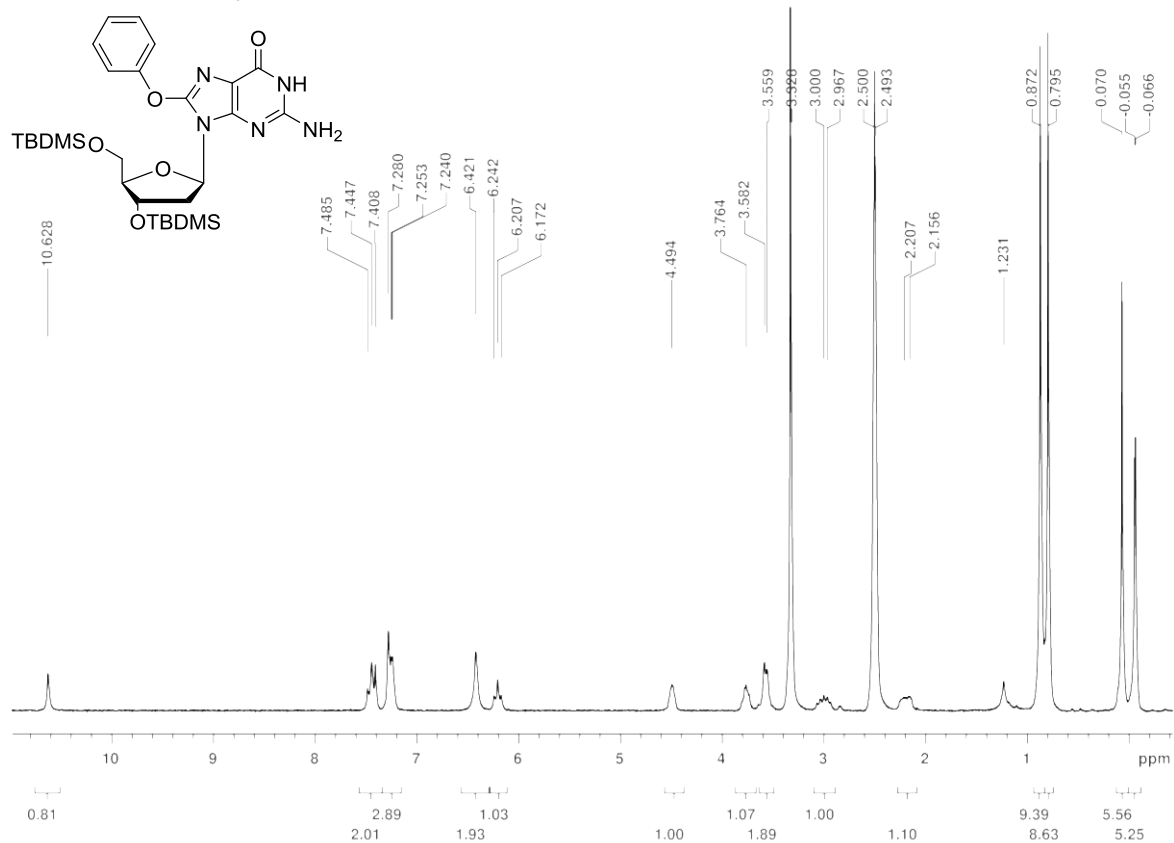
<sup>13</sup>C-NMR δ(dms<sub>o</sub>-d<sub>6</sub>): 14.413 (Me), 22.559 (-CH<sub>2</sub>-), 24.773 (-CO-CH<sub>2</sub>-CH<sub>2</sub>-), 28.868 (-CH<sub>2</sub>-), 29.139 (-CH<sub>2</sub>-), 29.168 (-CH<sub>2</sub>-), 29.318 (-CH<sub>2</sub>-), 29.417 (-CH<sub>2</sub>-), 29.464 (-CH<sub>2</sub>-), 29.486 (-CH<sub>2</sub>-), 29.501 (-CH<sub>2</sub>-), 31.759 (-CH<sub>2</sub>-), 33.892 (-CO-CH<sub>2</sub>-), 34.189 (C<sup>2'</sup>), 63.794 (C<sup>5'</sup>), 70.037 (CH- Fc-C<sub>5</sub>H<sub>5</sub>), 70.267 (CH- Fc-C<sub>5</sub>H<sub>4</sub>), 70.670 (C<sup>IV</sup> Fc), 71.900 (CH- Fc-C<sub>5</sub>H<sub>4</sub>), 74.567 (C<sup>3'</sup>), 81.765 (C<sup>4'</sup>), 82.519 (C<sup>1'</sup>), 111.305, 120.406 (*o*-CH-Ar), 125.752 (*p*-CH-Ar), 130.151 (*m*-CH-Ar), 149.411, 150.325, 153.915, 153.934 (C<sup>IV</sup> Ar), 156.320, 170.859 (CO-Fc), 173.040 (CO-CH<sub>2</sub>-) ppm.

Elemental analysis calcd (%) for C<sub>45</sub>H<sub>59</sub>FeN<sub>5</sub>O<sub>7</sub>: C 64.51, H 7.10, N 8.36; found: C 64.37, H 7.09, N 8.37.

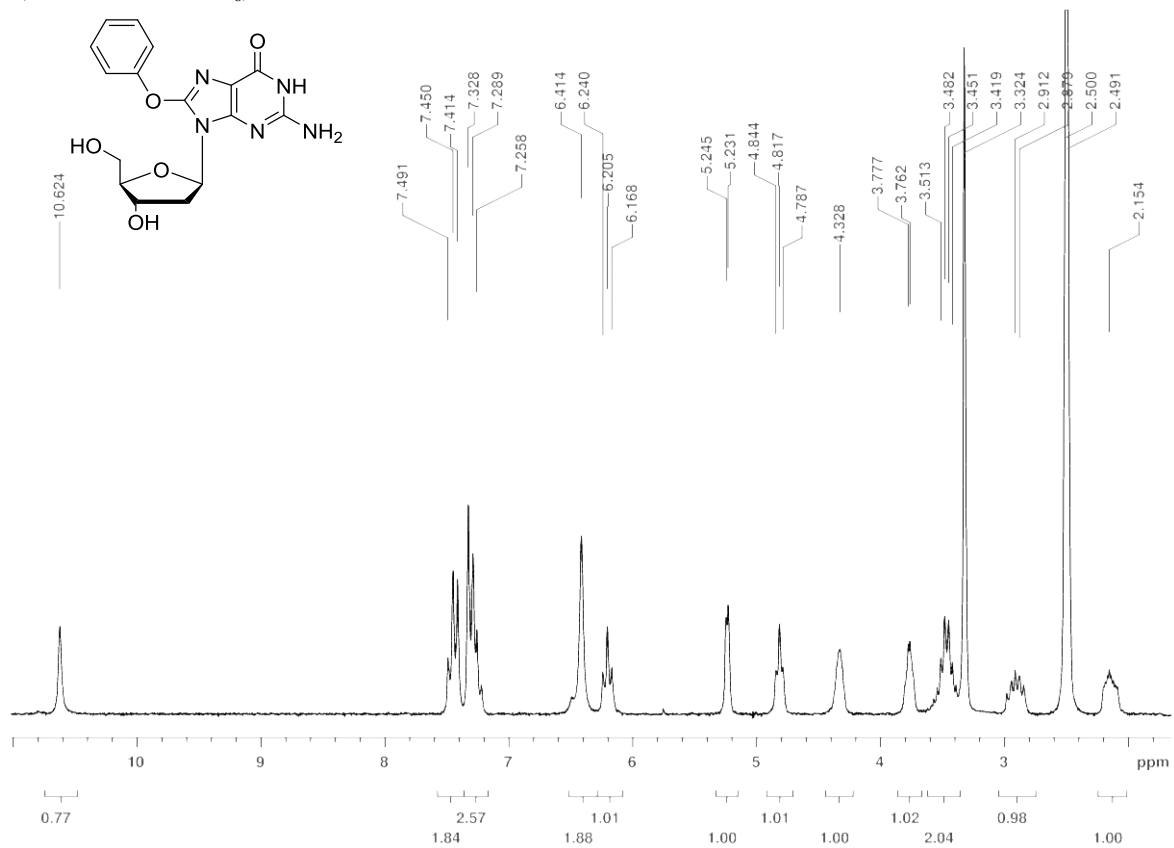
H-NMR (200 MHz DMSO-d<sub>6</sub>) of **9**



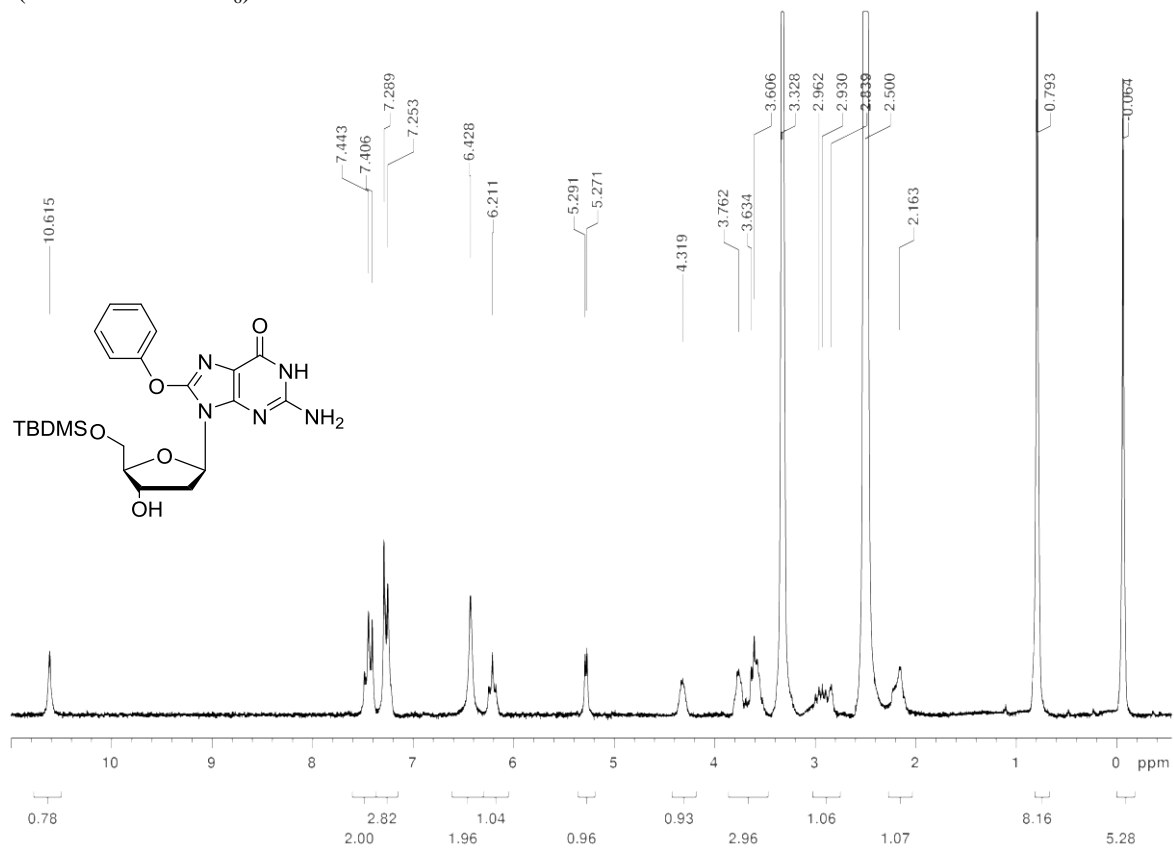
H-NMR (200 MHz DMSO-d<sub>6</sub>) of **10 a**



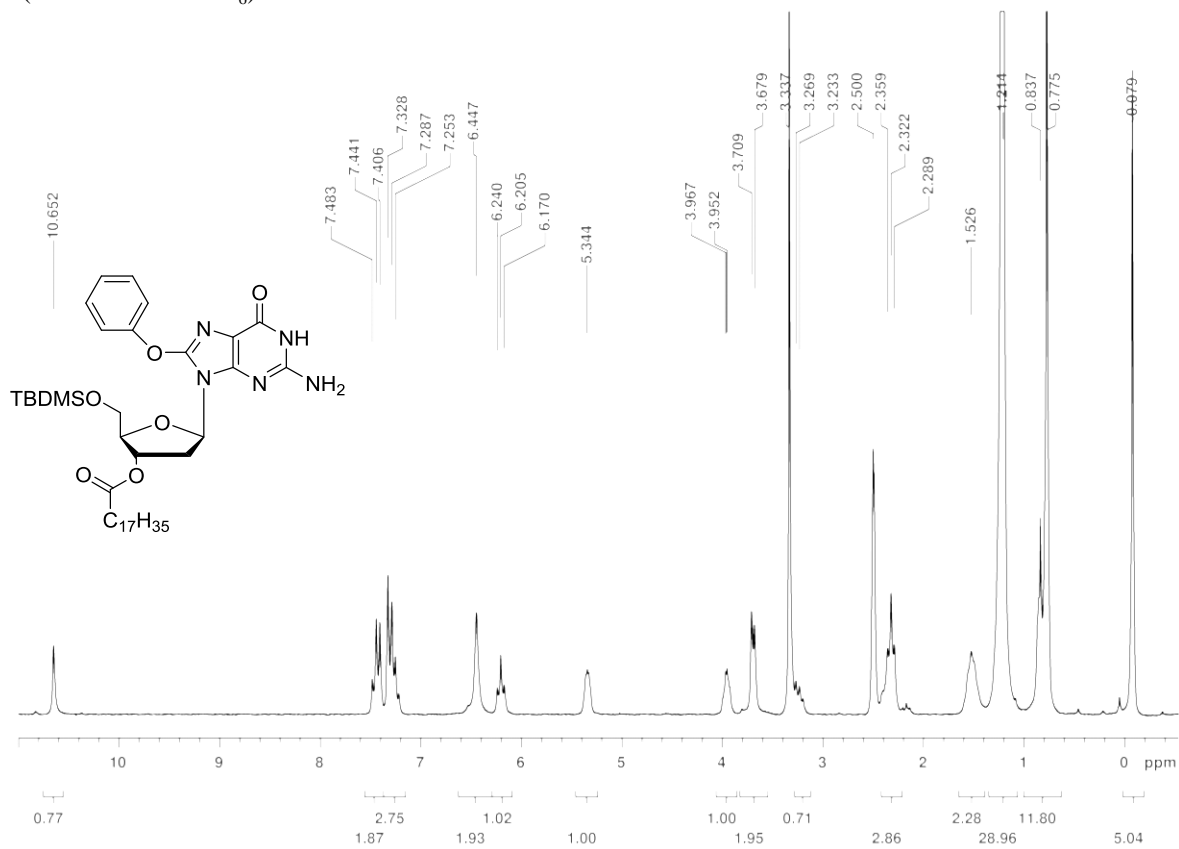
H-NMR (200 MHz DMSO-d<sub>6</sub>) of **10**



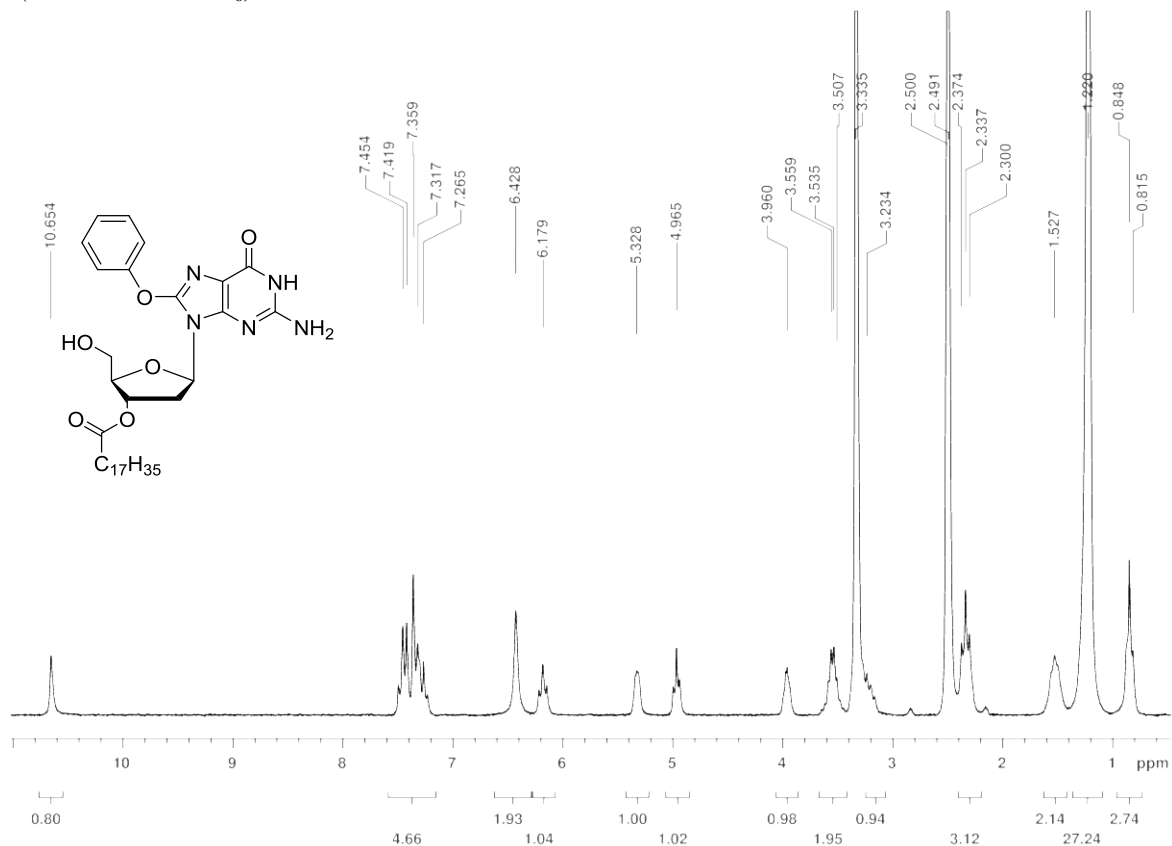
H-NMR (200 MHz DMSO-d<sub>6</sub>) of **11**



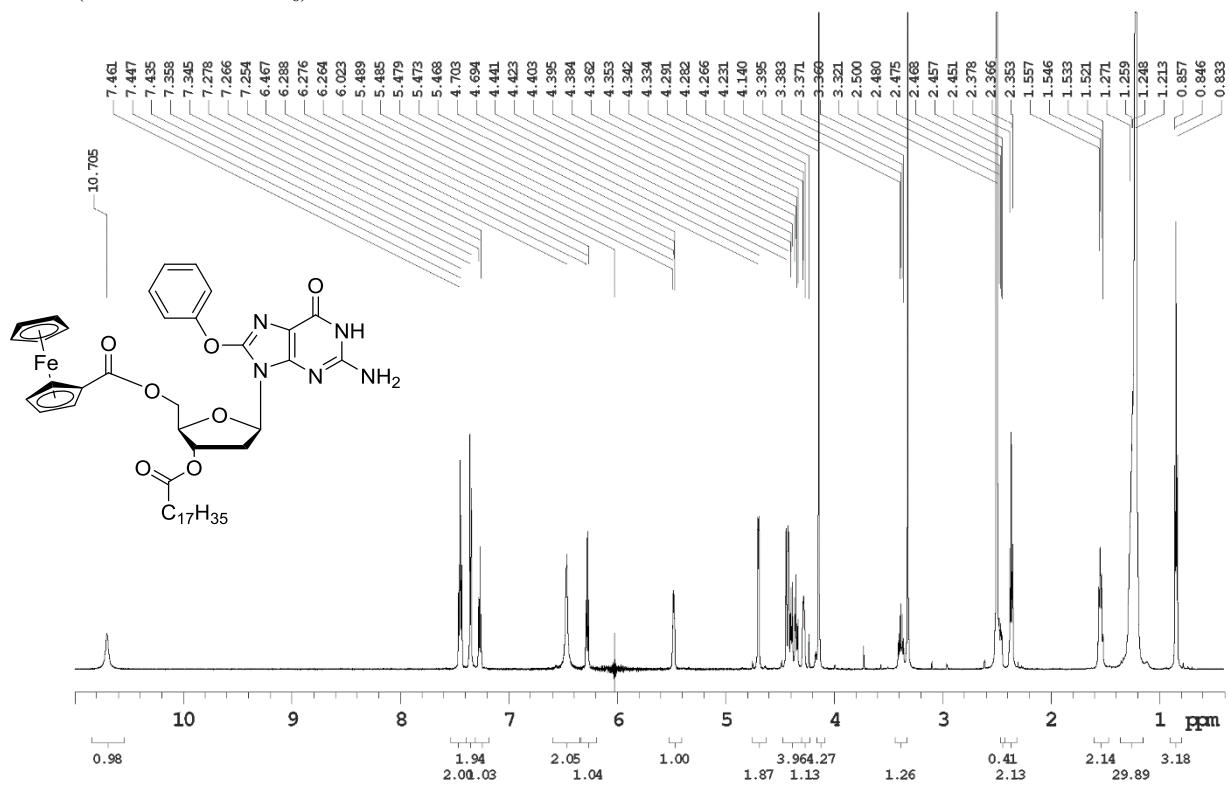
H-NMR (200 MHz DMSO-d<sub>6</sub>) of **12a**



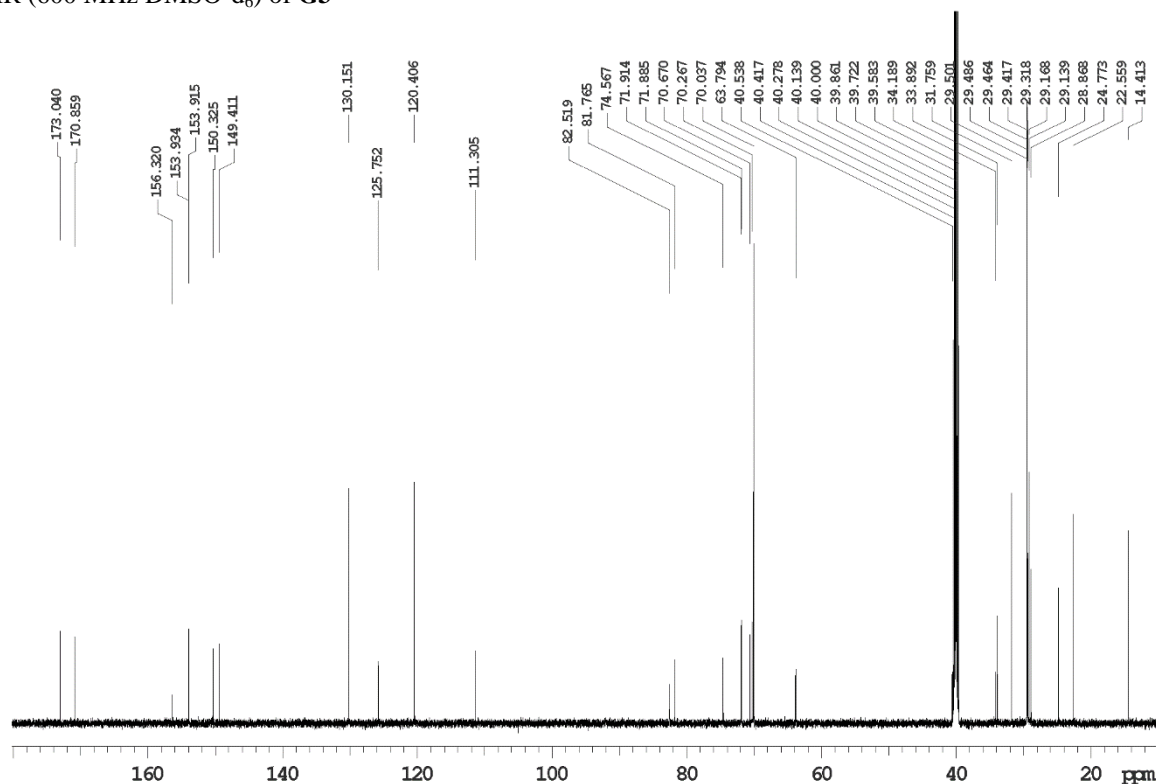
H-NMR (200 MHz DMSO-d<sub>6</sub>) of **12**



H-NMR (600 MHz DMSO-d<sub>6</sub>) of **G3**



$C^{13}$ -NMR (600 MHz DMSO- $d_6$ ) of G3



COSY-NMR (600 MHz DMSO- $d_6$ ) of G3

i600 std parameters

File: 8PhO\_d3\_3c18\_5Fc\_gCOSY\_dms0\_030914

Temp. 25.0 C / 298.1 K  
Operator: sangiac

Relax. delay 1.000 sec  
Acq. time 0.213 sec  
Width 9611.9 Hz  
2D Width 9611.9 Hz  
4 repetitions  
256 increments

OBSERVE H1, 599.7304216 MHz

DATA PROCESSING

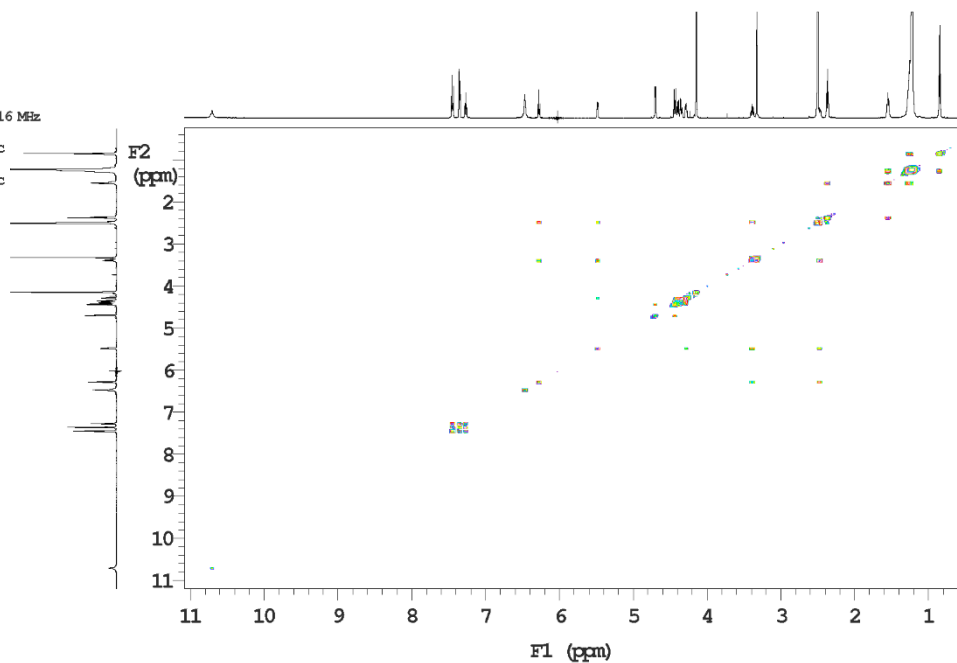
Sq. sine bell 0.107 sec

F1 DATA PROCESSING

Sq. sine bell 0.013 sec

FT size 4096 x 4096

Total time 0 min 0 sec



### HSQC -NMR (600 MHz DMSO-d<sub>6</sub>) of G3

i600 std parameters

File: 8PhO\_d3\_3C18\_5Fc\_gHSQCAD\_dms0\_030914

Temp. 25.0 C / 298.1 K  
Operator: sangiac

Relax. delay 1.000 sec  
Mixing 0.500 sec  
Acq. time 0.230 sec  
Width 9611.9 Hz  
2D Width 25632.8 Hz  
16 repetitions  
2 x 256 increments

OBSERVE H1, 599.7304206 MHz

DECOUPLE C13, 150.8136483 MHz

Power 43 dB

on during acquisition

off during delay

W40 Triple modulated

DATA PROCESSING

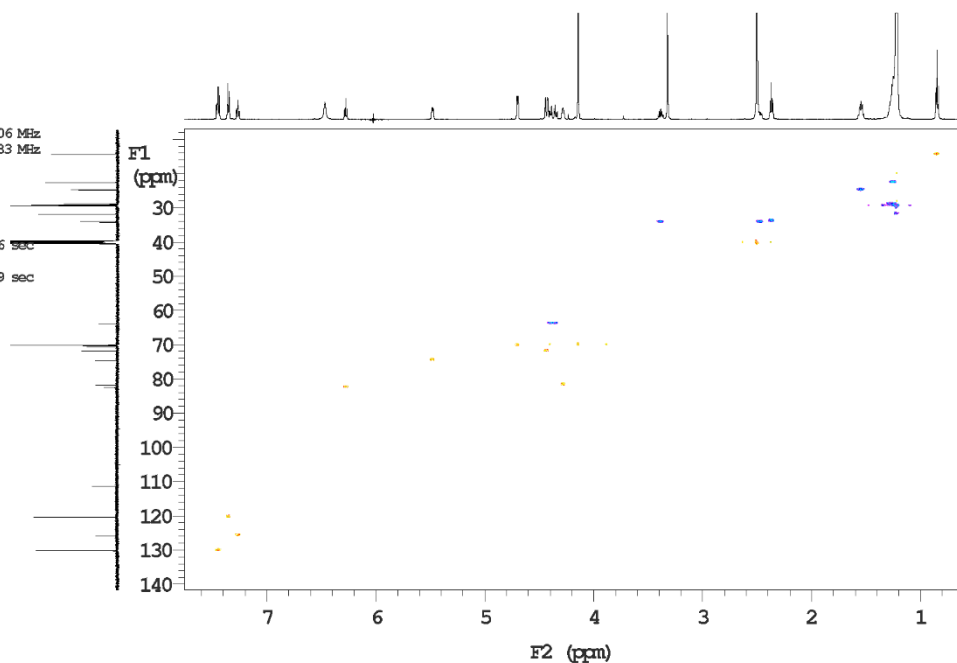
Gauss apodization 0.106 sec

F1 DATA PROCESSING

Gauss apodization 0.009 sec

FT size 8192 x 2048

Total time 0 min 0 sec



### HMBC -NMR (600 MHz DMSO-d<sub>6</sub>) of G3

i600 std parameters

File: 8PhO\_d3\_3C18\_5Fc\_gHMBC\_dms0\_030914

Temp. 25.0 C / 298.1 K  
Operator: sangiac

Relax. delay 1.000 sec  
Mixing 0.080 sec  
Acq. time 0.128 sec  
Width 9611.9 Hz  
2D Width 36199.1 Hz  
32 repetitions  
256 increments

OBSERVE H1, 599.7304239 MHz

DATA PROCESSING

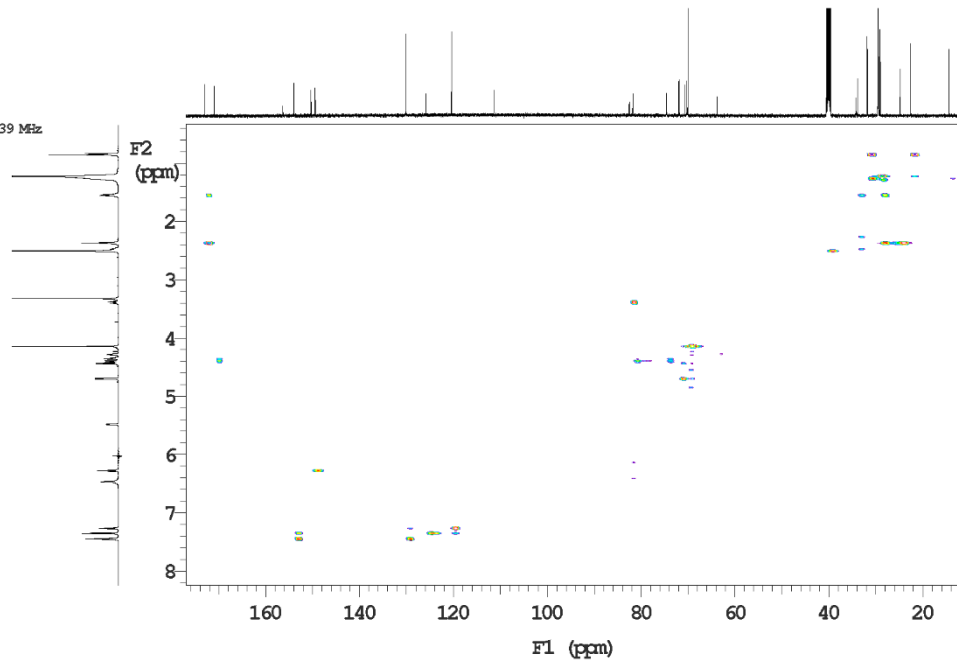
Sine ball 0.064 sec

F1 DATA PROCESSING

Sine ball 0.007 sec

FT size 4096 x 2048

Total time 0 min 0 sec



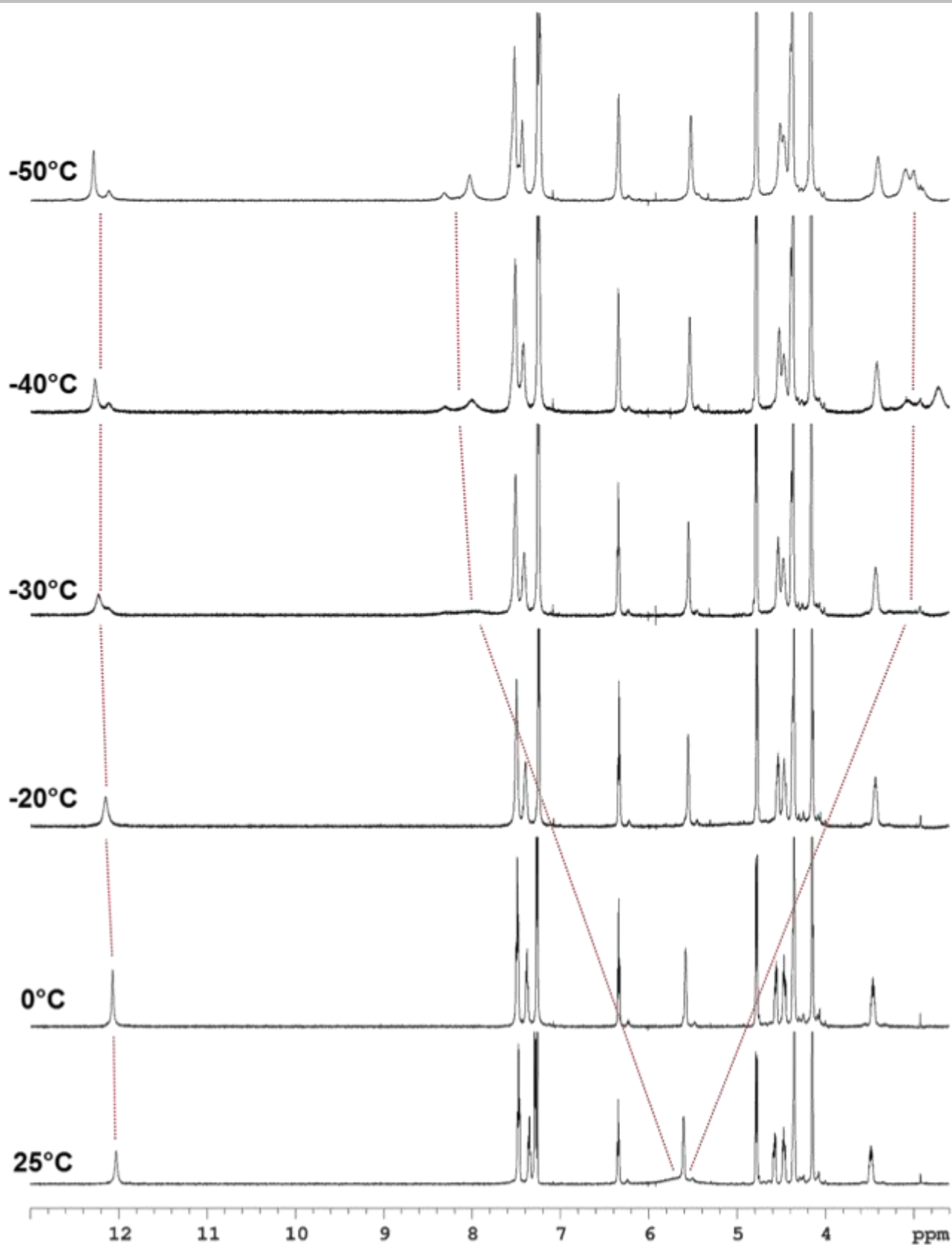


**Figure S5:** downfield portion of the <sup>1</sup>H-NMR spectrum of G3 (14 mM) at different temperatures in CDCl<sub>3</sub>. Guidelines highlight imino and amino N-H shifts.

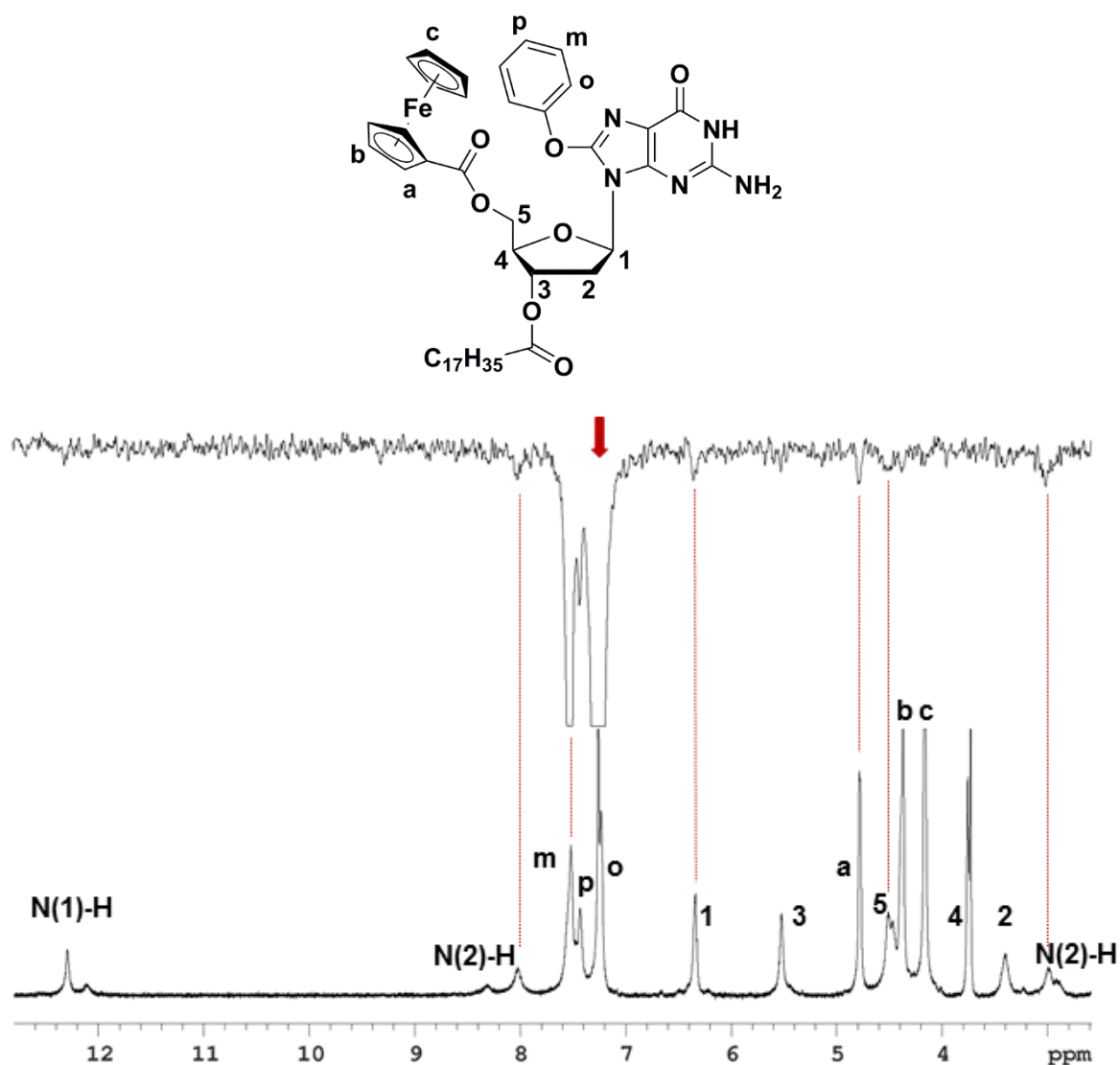


**Figure S6.** *Bottom:*  $^1\text{H-NMR}$  spectrum of **G3** in  $\text{CDCl}_3$  at  $-50^\circ\text{C}$ . Signals were assigned on the basis of COSY, HSQC and HMBC experiments. *Top:* noesy1d spectrum of the same sample (irradiation of protons **o** – see formula above – with a 50 Hz shaped pulse, mixing time 300 ms).

NOE spectra (Fig. S6) show weak contacts between ortho (**o**) and  $\text{H}_{1'}$  as well as between **o** and  $5'/5''$ : according to calculations, the two conformers differ only slightly in energy. In addition, NOE intermolecular proximities can be observed between **o** and ferrocene **a** and between **o** and both free N(2)-H and bound N(2)-H (major specie).

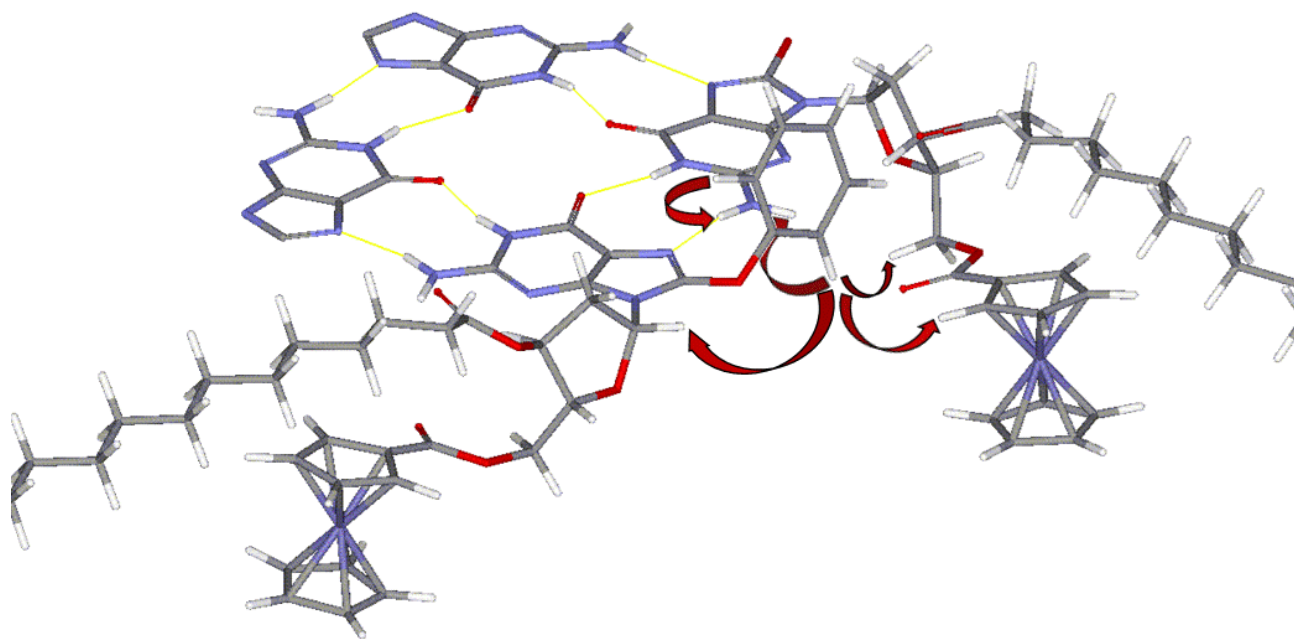


**Figure S7.** Model of an isolated G-quartet formed by *syn*-G3 (some atoms are omitted for clarity). NOE contacts of figure S6 are indicated by arrows.

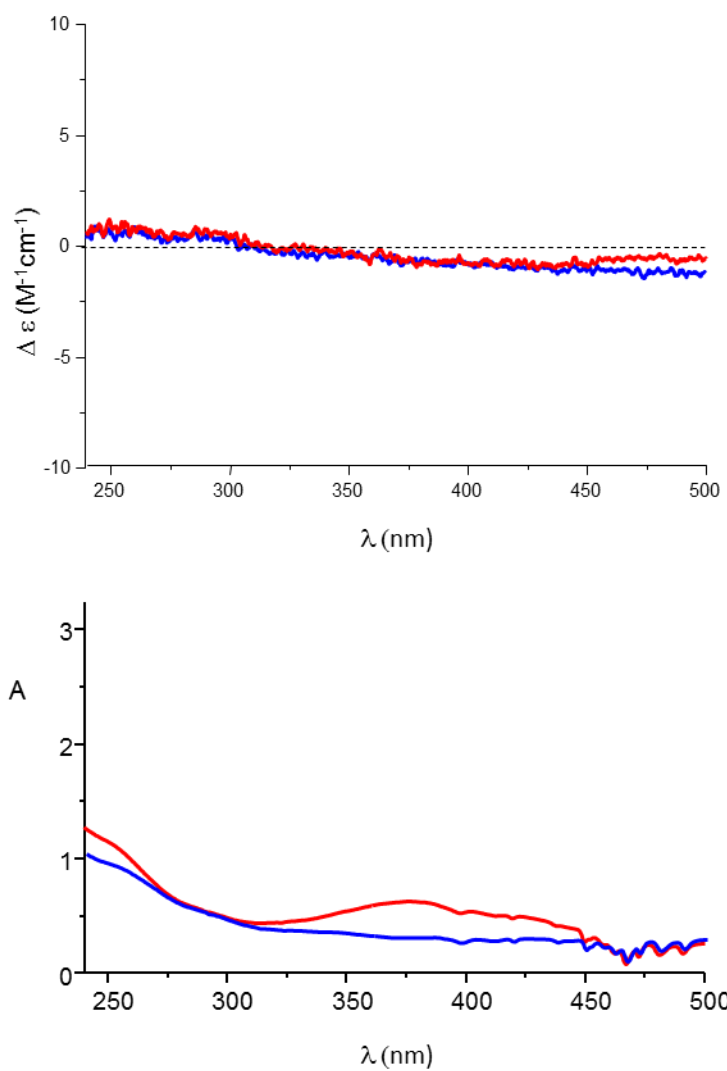


**Figure S8:** CD (top) and UV (bottom) spectra of **G3** (2.5 mM in  $CHCl_3$ ) before (blue) and after (red) addition of potassium picrate (1/8 mol/mol).

## 2. Scanning Tunneling Microscopy experiments

Scanning Tunneling Microscopy (STM) measurements were performed using a Veeco scanning Tunneling microscope (multimode Nanoscope III, Veeco) at the interface between a highly oriented pyrolytic graphite (HOPG) substrate and a supernatant solution, thereby mapping a maximum area of  $1\ \mu\text{m} \times 1\ \mu\text{m}$ . Solution of molecules were applied to the basal plane of the surface. For STM measurements, the substrates were glued to a magnetic disk and an electric contact was made with silver paint (Aldrich Chemicals). The STM tips were mechanically cut from a Pt/Ir wire (90/10, diameter 0.25 mm). The raw STM data were processed through the application of background flattening and the drift was corrected using the underlying graphite lattice as a reference. The lattice was visualized by lowering the bias voltage to 20 mV and raising the current up to 65 pA. STM imaging was carried out in constant height mode without turning off the feedback loop, to avoid tip crashes. Monolayer pattern formation was achieved by applying onto freshly cleaved HOPG 4  $\mu\text{L}$  of a solution. The STM images were recorded at room temperature once achieving a negligible thermal drift. Solutions of all molecules were prepared by dissolving the molecules in  $\text{CHCl}_3$  and diluting with 1-phenyloctane to give 1 mM solution (solvent composition 99 % 1-phenyloctane + 1 %  $\text{CHCl}_3$ ). All of the molecular models were minimized with MMFF and processed with QuteMol visualization software

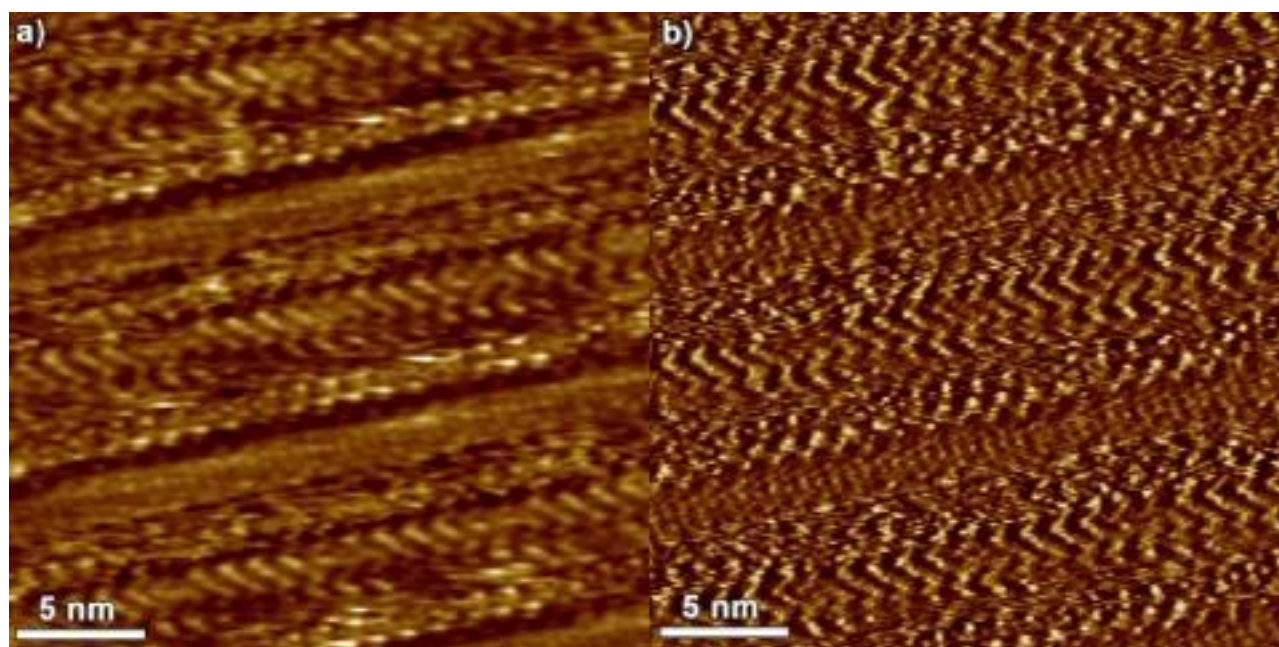


**Figure S9.** (a) Height and (b) current STM image of **G1** monolayer at the graphite-solution interface using 1-phenyloctane as a solvent. The image shows the supramolecular self-assembly forming ribbon-like structures of **G1**. Tunneling parameters:  $I_t = (35 \pm 2)$  pA,  $V_t = (400 \pm 25)$  mV.

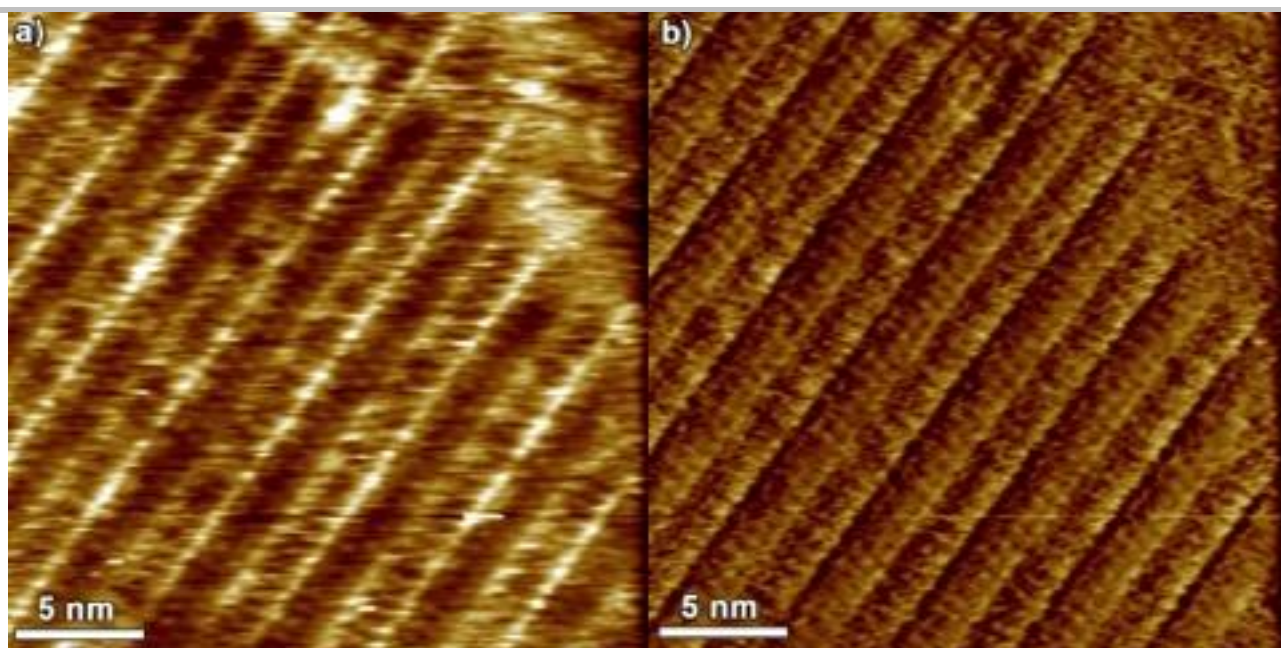


**Figure S10.** (a) Height and (b) current STM image of **G1** monolayer at the graphite-solution interface using 1-phenyloctane as a solvent. The image shows the supramolecular self-assembly forming ribbon-like structures of **G2**. Tunneling parameters:  $I_t = (35 \pm 2)$  pA,  $V_t = (400 \pm 25)$  mV.

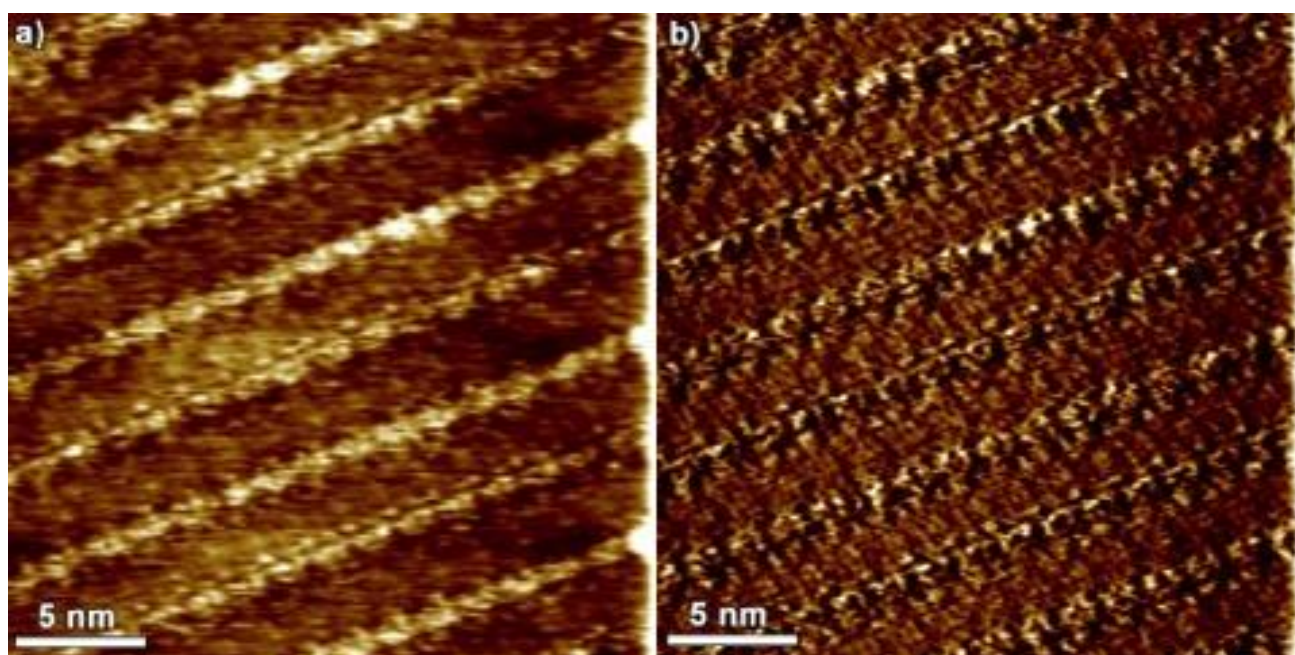


**Figure S11.** (a) Height and (b) current STM image of **G1** monolayer at the graphite-solution interface using 1-phenyloctane as a solvent. Tunneling parameters:  $I_t = (35 \pm 2)$  pA,  $V_t = (400 \pm 25)$  mV.

---

### 3. DFT calculations

To provide a molecular understanding of three **G** derivatives self-assembly in 2D and shed light onto the formation and stability of supramolecular structures, we have carried out density functional theory (DFT) calculations using the hybrid Gaussian and plane-wave method (GPW), implemented in the QUICKSTEP module of the CP2K package. We used the B3LYP hybrid exchange-correlation potential, whereas the Grimme's DFT-D2 method was employed for taking into account the dispersion forces. To gain insights into the intermolecular binding mechanisms, we have focused our attention on unravelling the interplay between H-bonds, which hold the guanine cores together, and the effective metallic repulsion coming from the four iron cations present in the ferrocenes. While the association energies have been discussed in the main text, in-depth discussion on electronic structure of all guanosine derivatives is presented in this section of ESI.

#### 3.1 Electronic structure of **G1**

The electronic structure of the **G1** (Fig. S12) displays interesting features due to hybridization between the metallic-like states associated to the d-like states provided by the ferrocene molecule and the  $\pi$ -states coming from the organic backbone. The interplay between these two-sets of orbitals leads to an overall delocalization of the molecular density over the whole complex where contributions of the metallic-like states can be spotted. In the upper orbitals (HOMO and HOMO-1) a strong contribution of the metallic-like states is observed, whereas a stronger contribution of the organic backbone is found in the HOMO-2 and HOMO-3 states. The *zig-zag* geometry observed in the formed ribbon leads to a configuration in which the ferrocene molecules are close to each other (10 Å) leading to a possible repulsive interaction due to the tendency of localization of charge in these complexes. In order to understand the mechanical stability of the complex, two different dimers have been studied, namely, a chain-chain dimer and a dimer composed as half of the ribbon.

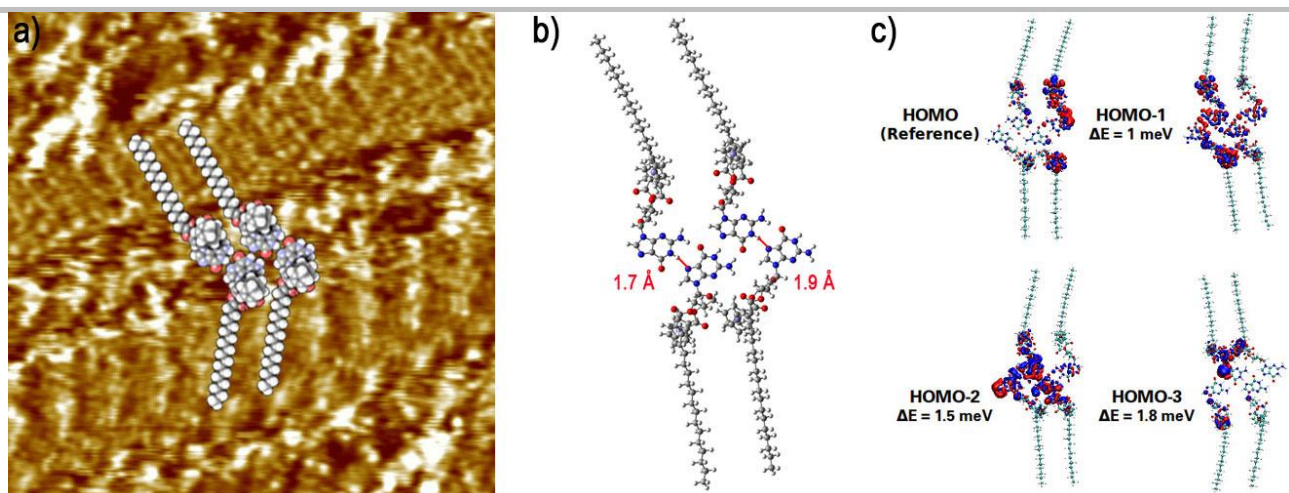


**Figure S12.** a) Molecular model for the **G1** ribbon overlaid STM image. b) Average distances in the relaxed structure. The calculated distances of the O-H and N-H atoms are 1.9 Å and 1.7 Å, respectively. For this configuration four different distances for the ferrocene molecules have been reported. Along the dimer formation, distances from 21.2 Å and 20.9 Å can be measured, whereas along the chain-chain dimer distances of 10.3 Å and 7.6 Å can be reported forming a rectangular-like shaped network. c) The first four molecular orbitals with the corresponding energy difference using HOMO energy as reference are displayed.

The molecular orbitals for both configurations have been calculated and the results shown in Figure S13 and Figure S14.

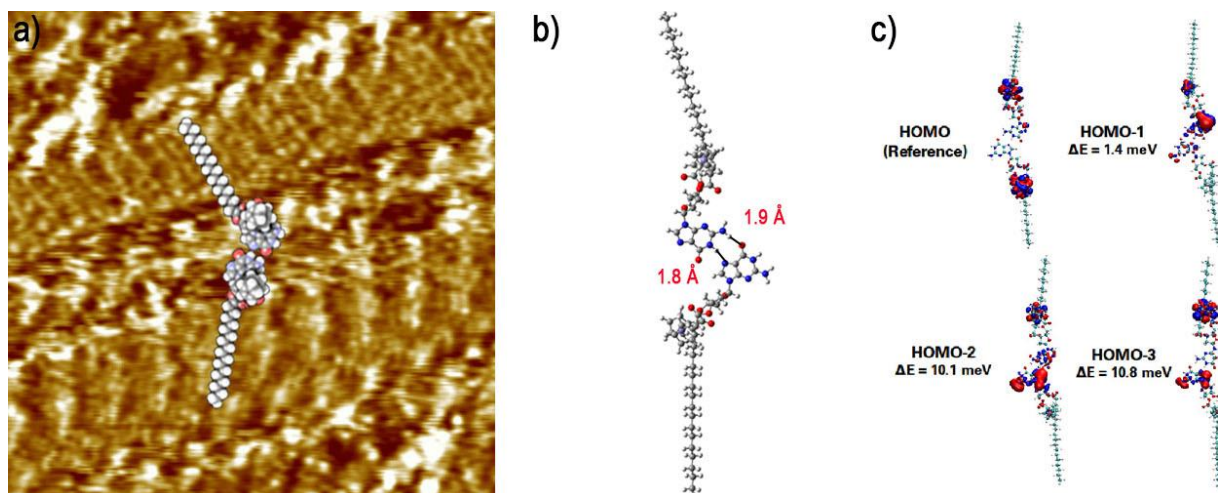


**Figure S13.** a) Molecular model for the **G1** ribbon dimer structure overlaid STM image. b) Average distance reported from the relaxed structure. The distances between the O-H and N-H atoms (black arrow and red arrows in the scheme) within the ribbon are 1.9 Å and 1.8 Å, respectively. The calculated distance for the Fe-Fe atoms is 26.5 Å. c) The first four molecular orbitals of the complex and its corresponding energy difference using HOMO energy as a reference are displayed.

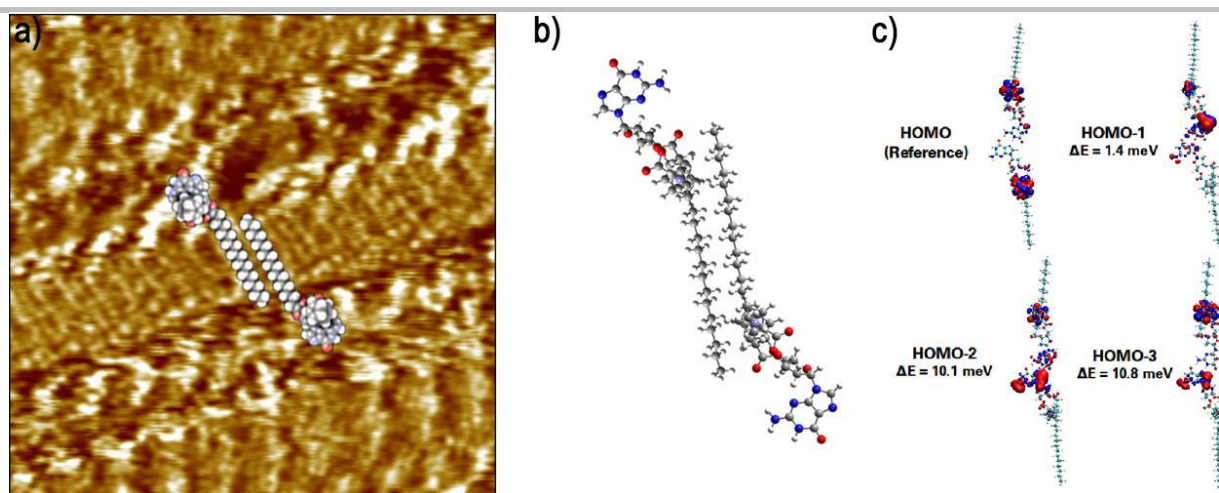


**Figure S14.** a) Molecular model for the **G1** chain-chain dimer structure overlaid STM image. b) Average distances reported from the relaxed structure. The reported distance between the C-C atoms (black arrow in the scheme) in the two long chains is 4.2 Å and the obtained distance for the Fe-Fe atoms is 13.9 Å. c) The first four molecular orbitals of the complex and its corresponding energy difference using HOMO energy as a reference are displayed.

In the case of the chain-chain dimer, the HOMO and HOMO-1 molecular orbitals display a stronger metallic nature than the HOMO-2 and HOMO-3 where a closer resemblance to the organic backbone orbitals can be observed. Likewise, for the dimer composed by half of the ribbon, the electronic structure depicts the same kind of organization as in the chain-chain case. The relaxed structures of the two dimers in which the ribbon can be dissociated give us information about the nature of the holding bond of each dimer. Thus, in the case of the chain-chain dimer, the reported distance between the carbon atoms within the chain corresponds to a VdW bond (4.2 Å), whereas the reported distances in dimer including part of the ribbon can be related to a H-bonding (1.8 Å and 1.9 Å). The hydrogen-bonding that holds the ribbon together can be described as the interaction of the NH<sub>2</sub> group with an oxygen atom localised in the opposite guanine while the second H-bonding takes place at a hydrogen atom (localised on the pentagon ring of the guanine) with a nitrogen atom localised at the hexagon ring in the guanine. Finally, in all cases, the reported energy difference between the HOMO-1, HOMO-2 and HOMO-3 with respect to the HOMO are of the order of few meV making all these states accessible at room temperature.

### 3.2 Electronic structure of **G2**

In the case of the **G2** ribbon the relaxed geometry and the resulting electronic structure are presented in Figure 15. The hybridization between the iron metallic-like states coming from the ferrocene and the pi-states provided by the organic backbone is also observed in this complex with the inclusion of some states belonging to the carbon chains, especially in the HOMO level. The HOMO-1 and HOMO-2 levels are where the metallic-like states are strongly observed in contrast to the HOMO and HOMO-3 where σ-like states are predominant. Energy differences between the

HOMO-1 to HOMO-3 with respect to the HOMO are all in the order of few meV, which is comparable with thermal energy, thus making most of these states accessible to the system at room temperature.

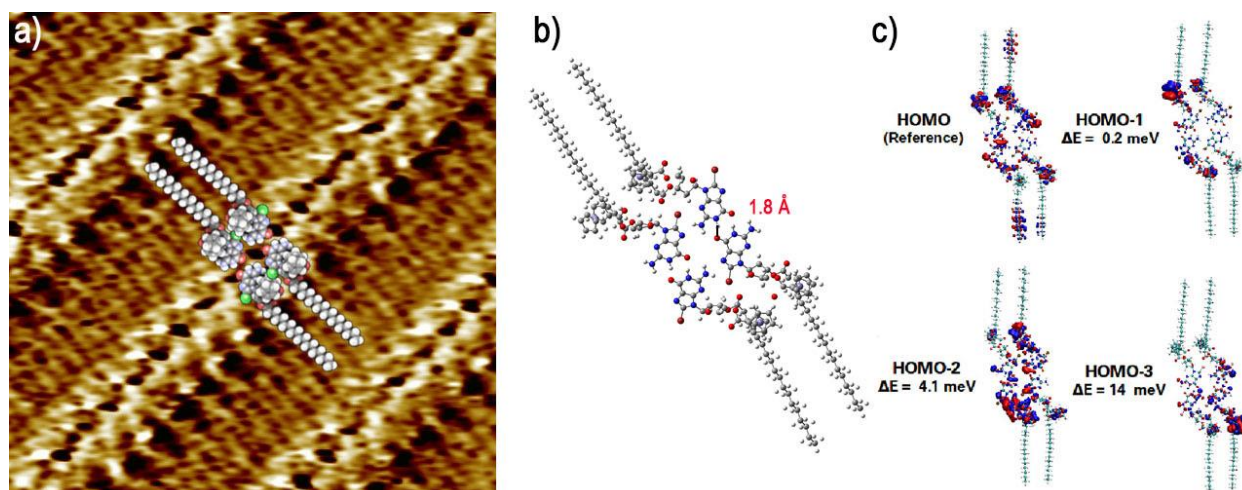


**Figure S15.** a) Molecular model for the **G2** ribbon. b) Average distance from the relaxed structure. The calculated distances of the O-H and N-H atoms are 1.9 Å and 1.7 Å, correspondingly. The obtained distance for the Br-H bonding is around 2.5 Å. For this configuration four different distances for the ferrocene molecules have been reported. Along the dimer formation, distances from 26.5 Å and 26.7 Å can be measured, whereas along the chain-chain dimer distances of 8.5 Å and 7.6 Å can be reported forming a rectangular-like shape network. c) The first four molecular orbitals with the corresponding energy difference using HOMO energy as reference are displayed.

Finally, it is worth to notice that in this complex, besides the hydrogen bonding observed between the oxygen and hydrogen atoms belonging to the guanine complexes (around 1.8 Å), the inclusion of bromine opens the opportunity to have a halogen bonding that also participates in the formation of the ribbon. However, in the calculated molecular orbitals there is no a clear fingerprint that indicates that bromine contributes significantly to the valence states of the molecule or forms any halogen bond, but rather, it is coupled with the hydrogen atom of the opposite guanine molecule. Likewise, it is interesting to notice that the calculated distance between the iron atoms belonging to the ferrocene molecules along the bromine direction are the smallest reported in these three complexes.

This is an important issue in the overall mechanical stability of the system since effective Coulomb repulsion between localised states like HOMO-1 and HOMO-3 and source of mechanical instabilities that are smoothed by either the long distance between the ferrocene molecules where the localisation of charge occurs or by the H-bonding holding the ribbons. In the case of the ribbon dimer, the calculated molecular orbitals show a stronger hybridization between the  $\pi$ -states associated to the organic backbone and the d-states coming from the ferrocene resulting in the spreading of the molecular orbitals over the whole complex. The obtained structure suggests a

picture of double hydrogen bonding in which the oxygen atom belonging to the hexagonal ring in one of the guanines is coupled to the hydrogen atom belonging to the hexagon in the opposite guanine molecule. This H-bonding is a totally different one as that observed in the previous case where the coupling was achieved by the interaction of one oxygen atom to the hydrogen belonging to the NH<sub>2</sub> molecule demonstrating the versatility of these complexes to form ribbons *via* H-bonding networks. Finally, the difference in energies between the HOMO-1, HOMO-2 and HOMO-3 to the HOMO is again of the order of only few.

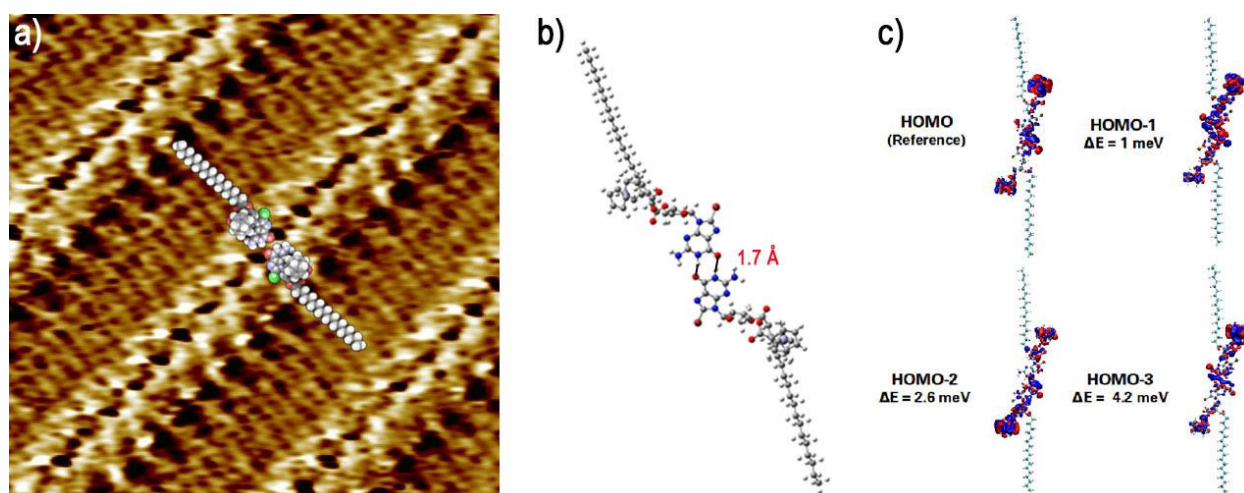


**Figure S16.** a) Molecular model for the **G2** ribbon structure. b) Average distance reported from the relaxed structure. The distances between the O-H and N-H atoms (black arrow and red arrows in the scheme) within the ribbon are 1.9 Å and 1.8 Å, respectively. The calculated distance for the Fe-Fe atoms is 26.5 Å. c) The first four molecular orbitals of the complex and its corresponding energy difference using HOMO energy as a reference are displayed.

The electronic structure of the chain-chain dimer (Fig. S17) indicates that charge localization in the ferrocene is more favorable in the case of the lower molecular orbitals (HOMO-2 and HOMO-3) than in the upper molecular orbitals (HOMO and HOMO-1). According to our results, the chains are playing a more active role in the complex contributing in the overall molecular orbitals in the case of HOMO and HOMO-1 while maintaining the same distance as reported in the previous complex suggesting still a vdW bonding (4.2 Å). The obtained distances between iron ions placed at the ferrocene complexes have been increased around 5 Å with respect to the **G2** case. This fact allows us to state that the effective Coulomb repulsion due to localised states within these molecules is smaller than in the previous case. The difference in energies between the HOMO-2, HOMO-3 and HOMO-1 with respect to the HOMO energy used as references remains of the same order of a few meV.

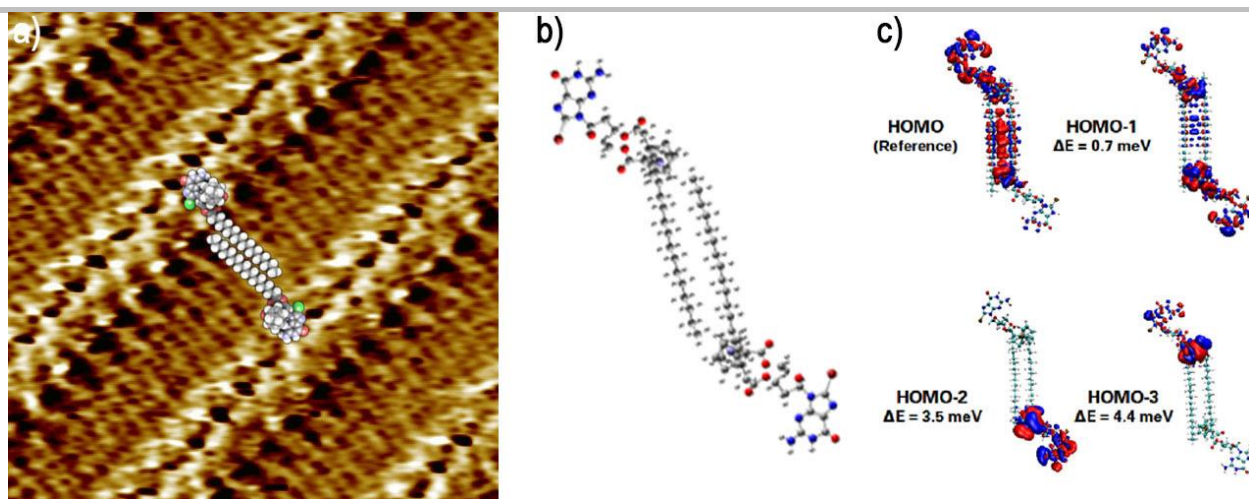


**Figure S17.** a) Molecular model for the chain-chain **G2** dimer. b) Average distance from the relaxed structure. The reported distance between the C-C atoms (black arrow in the scheme) in the two long chains is 4.2 Å and the obtained distance between the Fe-Fe atoms is 17.5 Å. c) The first four molecular orbitals of the complex and its corresponding energy difference using HOMO energy as a reference are displayed.

### 3.3 Electronic structure of **G3**

The geometry optimized structure for the **G3** structure is presented in Figure S18. In contrast to the other cases, the phenyl groups play an important role in the overall geometry organization within the complex since its arrangement displays an inclination when compared to the plane defined by the ribbon as has been suggested in the schematic molecular model built from the STM images and subsequently confirmed by the DFT calculations. This rearrangement of atoms within the ribbon not only possibly reduces the extra tension generated by the inclusion of the phenyl group in the guanine molecule, but also favours the preservation of ribbon structure formed by the H-bonding between the different guanine complexes. Moreover, the reported distances between the ferrocene molecules within the complex are still in the same order of magnitude than the other two complexes. Similarly to the other complexes the hybridization of molecular states take place between the metallic-like states coming from the ferrocene molecule with the pi-states provided by the backbone with some spatial extension over the phenol group.

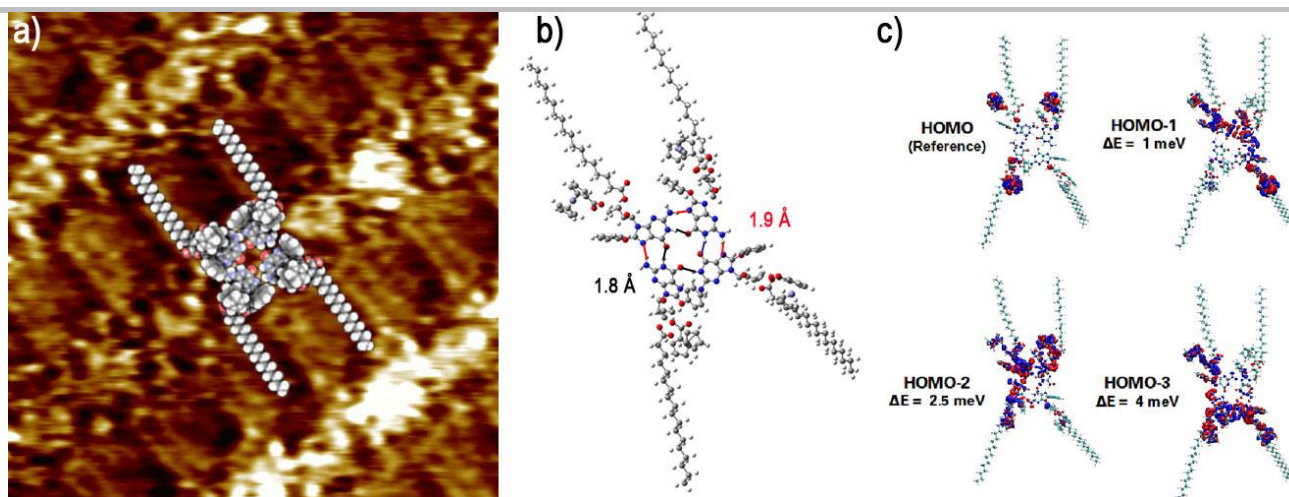


**Figure S18.** (a) Molecular model for the **G3<sub>4</sub>**. (b) Average distance from the relaxed structure. The calculated distance of the O-H and N-H atoms are 1.9 Å and 1.8 Å, respectively. For this configuration four different distances for the ferrocene molecules have been reported. Along the dimer formation, distances from 25.7 Å and 25.3 Å can be reported, whereas along the chain-chain dimer distances of 16.6 Å and 17.1 Å can be stated. The configuration forms a rectangular-like shape network. (c) The first four molecular orbitals with its corresponding energy difference using HOMO energy as reference are presented.

As in the previous cases, the two possible dimers in which the quartet can be decomposed are presented in Figure S19 and S20. In the dimer that contains half of the ribbon structure is not only observed the usual hybridization between metallic-like and  $\pi$ -like molecular orbitals (HOMO-2 and HOMO-3) but also contribution in the molecular orbitals (HOMO and HOMO-1) of atoms coming from the alkyl chains. The reported distances of the N-H and O-H atoms are in agreement with the usual distances for the H-bonding (1.9 Å and 1.8 Å), while the distances between the iron atoms in the ferrocene molecule are around 25.6 Å. In the case of the chain-chain dimer, the calculated electronic structure suggest a stronger hybridization of the metallic-like and  $\pi$ -states molecular orbitals coming from the ferrocenes and the organic backbone of the molecule, respectively in the HOMO, HOMO-1 and HOMO-4, while in the HOMO-3 a strong metallic-like state is found. Although we find bigger energy differences between the molecular orbitals with respect to the HOMO, they are still energetically close enough to make all of them accessible at room temperature.

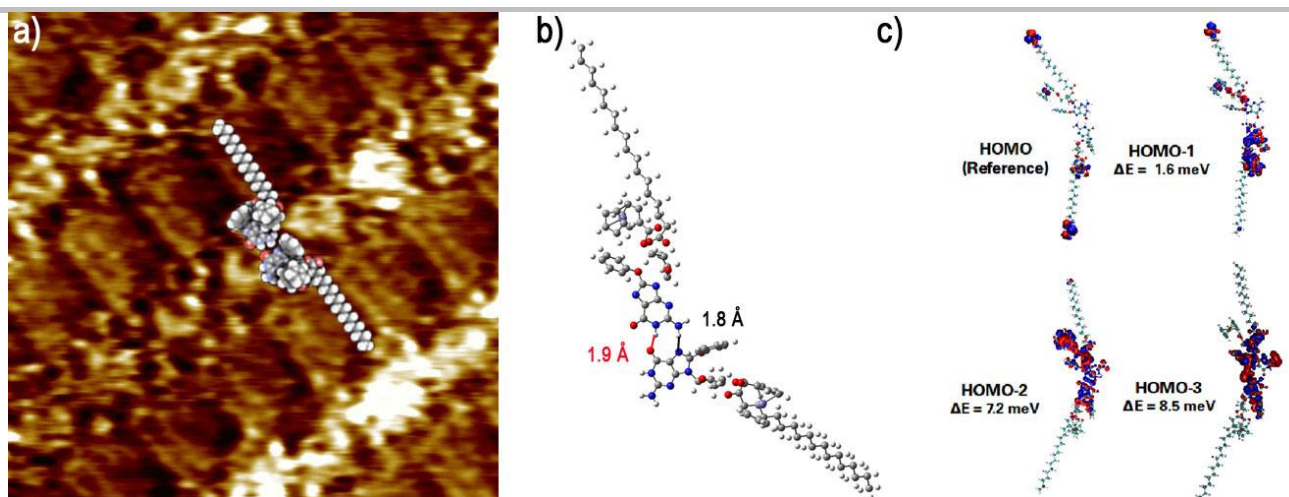


**Figure S19.** a) Molecular model for the  $G3_2$ . b) Average distance reported from the relaxed structure. The distances between the O-H and N-H atoms (black arrow and red arrows in the scheme) within the ribbon are 1.9 Å and 1.8 Å, respectively. The calculated distance for the Fe-Fe atoms is 25.6 Å. c) The first four molecular orbitals of the complex and its corresponding energy difference using HOMO energy as a reference are displayed.

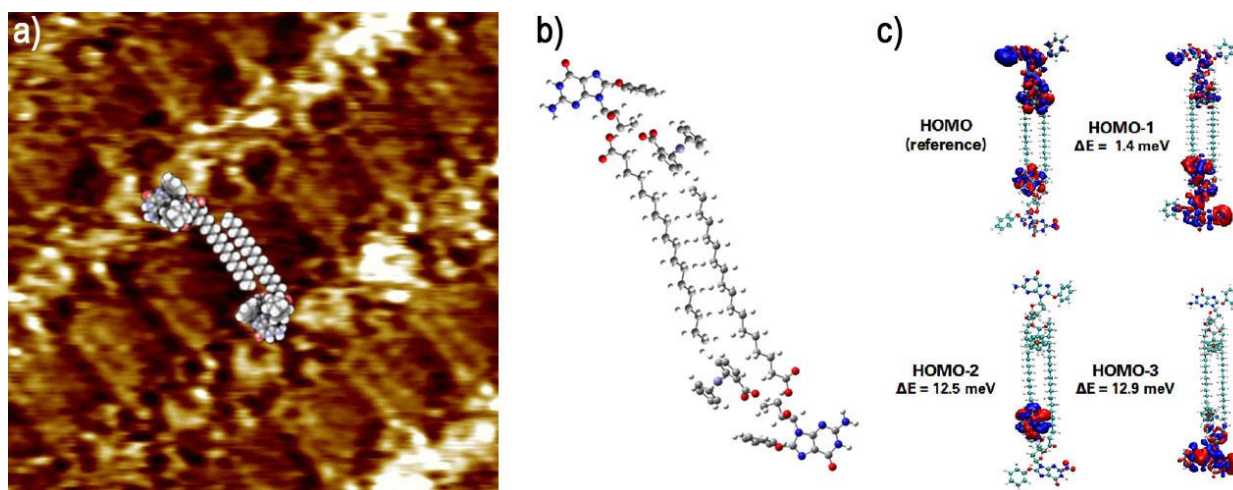


**Figure S20.** a) Molecular model for the chain-chain  $G3_2$  dimer. b) Average distance reported from the relaxed structure. The distance between the C-C atoms (black arrow in the scheme) in the two long chains is around 3.9 Å. The obtained distance for the Fe-Fe atoms is 16.2 Å. c) The first four molecular orbitals of the complex and its corresponding energy difference using the HOMO energy as a reference are displayed.

#### References:

- [1] Hutter, J; Iannuzzi, M; Schiffmann, F; VandeVondele, J. Wiley Interdisciplinary Reviews-Computational Molecular Science, 4 (1), 15-25 (2014).
- [2] VandeVondele, J; Hutter, J.; J. Chem. Phys., 127 (11), 114105 (2007).
- [3] Frigo, M; Johnson, SG. Proceedings of the IEE, 93 (2), 216-231 (2005).
- [4] VandeVondele, J; Hutter, J.; J. Chem. Phys., 118 (10), 4365-4369 (2003).
- [5] Lippert, G; Hutter, J; Parrinello, M. Theor. Chem. Acc., 103 (2), 124-140 (1999).
- [6] Krack, M; Parrinello, M. PCCP, 2 (10), 2105-2112 (2000).
- [7] Becke, AD. Phys. Rev. A, 38 (6), 3098-3100 (1988).
- [8] Lee, CT; Yang, WT; Parr, RG. Phys. Rev. B, 37 (2), 785-789 (1988).
- [9] Vosko, SH; Wilk, L; Nusair, M. Canadian Journal of Physics, 58 (8), 1200-1211 (1980).